(Invitrogen) according to the manufacturer's instructions in 100 µl/well Opti-MEM (Invitrogen). AMO concentrations varied as indicated, whereas plasmid concentrations remained constant at 0.1 µg/well. After 6 h of transfection, cells were re-fed with complete media. Cells were lysed at indicated hours after transfection, and luciferase activities were measured using the Dual-Luciferase Reporter Assay System (Promega). Relative firefly luciferase signals were normalized against *Renilla* luciferase signals. Results are expressed as relative Fluc/Rluc ratios to that of mirGLO-treated cells. Each experiment was performed at least three times.

Preparation of AMO encapsulated liposome

As a liposomal delivery system, YSK05-MENDs encapsulating AMOs were prepared by a *t*-BuOH dilution procedure (30,31). Thus, each AMO was mixed with 90% (v/v) *t*-BuOH containing YSK05 (synthesized as previously described) (30), cholesterol (Avanti Polar Lipid), 1,2-dimyristoyl-sn-glycerol and methoxyethyleneglycol 2000 ether (Avanti Polar Lipid) at a molar ratio of 70:30:3 in 20 mM citrate buffer (pH 4.0) at AMO/lipids of 0.1 (wt/wt) under strong agitation to a *t*-BuOH concentration of 60% (v/v). Then, lipids/AMO mixture was added into 20 mM citrate buffer (pH 4.0) under strong agitation to a *t*-BuOH concentration of <12% (v/v). Ultrafiltration was performed to remove *t*-BuOH, replace external buffer with phosphate buffered saline (PBS, pH 7.0) and concentrate a resulting YSK05-MEND encapsulating AMO (AMO-YSK05-MEND). The average diameter and zeta-potential of the AMO-YSK05-MENDs were determined using a Zetasizer Nano ZS ZEN3600 (MALVERN Instrument, Worchestershire).

In vivo experiments

Female BALB/c mice (8 weeks old) were purchased from Japan SLC. All *in vivo* experiments were approved by the Institutional Animal Care and Use Committee. One day before the administration, serum was collected for measuring cholesterol concentration. Each AMO-YSK05-MEND was diluted to the appropriate concentrations in PBS (pH 7.4), followed by intravenous administration via the tail vein at a dose of 1 mg AMO/kg in 10 ~ 15 ml/kg given once a day, every other day, for three times. At 48 h after the last injection, liver and blood were collected. Blood sample was centrifuged at 8*g* at 4°C for 5 min to obtain plasma. To obtain serum, blood sample was stored overnight at 4°C, followed by centrifugation (10 000 rpm, 4°C, 10 min). Cholesterol concentration in plasma and alanine aminotransferase level in serum were determined using a cholesterol E-test WAKO and Transaminase CII-test WAKO (Wako) according to the manufacturer's protocols. Total RNAs in liver were isolated using TRIzol (Invitrogen) according to the manufacturer's protocols. Then, isolated RNAs were reverse transcribed using a High Capacity RNA-to-cDNA kit (Applied Biosystems) according to manufacturer's protocol. A quantitative polymerase chain reaction (PCR) analysis was performed with 20 ng of cDNA using Fast SYBR Green Master Mix (Applied Biosystems) on the Lightcycler480 System II (Roche Applied Science). All reactions were performed at a volume of 15 µl. The primers for qRT-PCR are as follows: mouse AldoA (forward) 5′-GATGGGTCCAGC TTCAAC-3′ and (reverse) 5′-GTGCTTTCCTTTCCTAA CTCTG-3′; mouse Bckdk (forward) 5′-AGGACCTATG CATGGCTTTG-3′ and (reverse) 5′-CCGTAGGTAGAC ATCCGTG-3′; mouse Ndrg3 (forward) 5′-ATGGGCTA CATACCATCTGC-3′ and (reverse) 5′-TCTGACTGATT GCTGGTCAC-3′; mouse Hprt1 (forward) 5′-CGTGATT AGCGATGATGAAC-3′ and (reverse) 5′-GCAAGTCTT TCAGTCCTGTC-3′. Each data was normalized by Hprt1 expression. All experiments were performed in triplicate and data show mean values from at least three assays.

Statistical analysis

Comparisons between multiple treatments were made using one-way analysis of variance (ANOVA), followed by the SNK test. Pair-wise comparisons between treatments were made using a student's *t*-test. $P < 0.05$ was considered significantly different.

RESULTS AND DISCUSSION

Evaluation of inhibitory activity of AMOs against miR-21

We first synthesized modified AMOs against miR-21, a miRNA that is overexpressed in many tumors and thus is considered to be a potential therapeutic target in oncology (32). The sequences and modification patterns of AMOs were shown in Table 1. Because 2′-F-4′-thioRNA showed highest hybridization ability with its complementary RNA among the chemically modified ONs tested (21,33), we synthesized chimeric 2′-OMe-4′-thio/2′-F-4′-thio–modified AMOs (AM21SMF1 and AM21SMF2) along with 2′-OMe-4′-thio–modified AMO (AM21SM), which are complementary and the same length (22-mer) as mature miR-21. For comparison, 4′-oxo congeners (AM21M, AM21MF1 and AM21MF2) were also prepared. Because Hutvagner *et al.* reported that AMOs possessing a complementary sequence core with 5 nt flanking sequences on both 5′- and 3′-ends showed more potent anti-miRNA activity (19), we also designed a 32-mer uniformly 2′-OMe-4′-thioribonucleoside–modified AMO (AM21SM-L), which exhibits perfect complimentarity to miR-21 and 5 nt flanking regions on both ends, as well as that of 2′-OMe (AM21M-L).

To evaluate anti-miRNA activity of the synthetic AMOs, we constructed a miR-21 luciferase reporter plasmid (34), which has two perfectly matched miR-21 binding sites arranged in tandem on 3′UTR of firefly luciferase gene (pmirGLO21). The firefly luciferase activity was completely suppressed (3.7%) when the pmirGLO21 was transfected into HeLa cells, a cell line known to have high endogenous levels of miR-21 (Figure 2). The activity of pmirGLO, which has no miR-21 binding sites, was high (normalized as 100%) on transfection into HeLa cells. Our hypothesis is that introduction of miR-21 AMO can prevent miR-21 binding to the pmirGLO21 target sites, resulting in increased

Table 1. Sequence and modification patterns of anti-miR-21 AMOs

AMO	Sequence[a]	T_m (°C)[b]
AM21SM	5′-**UCAACAUCAGUCUGAUAAGCUA**-3′	64.1
AM21SMF1	5′-**ucAAcAucAGucuGAuAAGcuA**-3′	69.2
AM21SMF2	5′-**UCaacaucagucugauaagcUA**-3′	71.1
AM21M	5′-UCAACAUCAGUCUGAUAAGCUA-3′	59.9
AM21MF1	5′-ucAAcAucAGucuGAuAAGcuA-3′	64.2
AM21MF2	5′-UCaacaucagucugauaagcUA-3′	67.9
AM21SM-L	5′-**UCUUAUCAACAUCAGUCUGAUAAGCUAACCUU**-3′	62.1
AM21M-L	5′-UCUUAUCAACAUCAGUCUGAUAAGCUAACCUU-3′	58.0

[a]Uppercase letters represent 2′-OMe; lowercase letters represent 2′-F; bold uppercase letters are 2′-OMe-4′-thioribonucleotides; bold lowercase letters are 2′-F-4′-thioribonucleotides, [b]T_ms were measured versus with target miR-21 (22-mer) in a phosphate buffer (10 mM, pH 7.0) containing 0.1 mM EDTA and 1 mM NaCl, 3 μM strand concentration. Values were given as an average of three independent experiments.

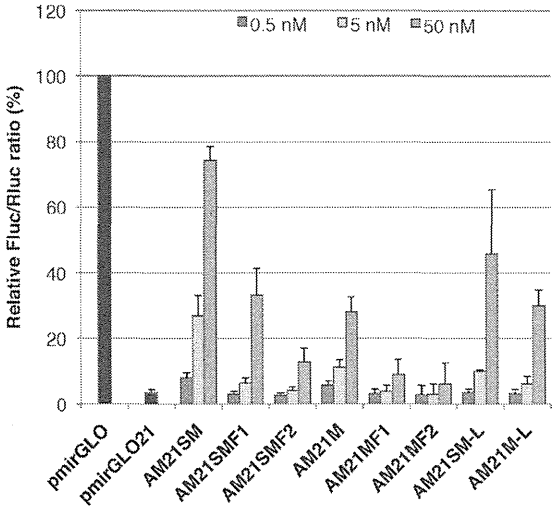

Figure 2. Anti-miR-21 activity of modified AMOs. HeLa cells were co-transfected with the miR-21 reporter plasmid (mirGLO21) and the indicated modified anti-miR-21 AMOs at the indicated concentrations. The dual luciferase assay was performed at 24 h after transfection. Data are shown as mean with standard deviation (SD).

luciferase expression by either causing translational inhibition or cleavage of the mRNA. We then tested anti-miRNA activity of AMOs. As shown in Figure 2, all our AMOs showed miR-21 inhibitory activity in a dose-dependent manner. In general, 4′-thio–modified AMOs (AM21SM, AM21SMF1 and AM21SMF2) showed much higher activity than 4′-oxo congeners (AM21M, AM21MF1 and AM21MF2). The activities of chimera AMOs (AM21SMF1, AM21SMF2, AM21MF1 and AM21MF2) were less effective compared with uniformly modified AMOs (AM21SM and AM21M). Contrary to the results reported by Hutvanger *et al.* (19), no significant improvement was observed in 32-mer AM21M-L (30.0% at 50 nM) compared with 22-mer AM21M (27.9% at 50 nM). Furthermore, among the AMOs tested, the shorter AMO, namely AM21SM, was more potent than AM21SM-L (74.3 and 45.9%, respectively) in the case of 4′-thio–modified AMOs. The highest activity was observed with AM21SM, with a luciferase level of 74.3% at 50 nM, which was >2.5 times as much as that of AM21M (27.9% at 50 nM).

It is known that there is a good correlation between T_m value of AMOs and *in vitro* potency (35). Therefore, we compared the thermal stability of the AMOs with target miR-21 based on their T_m values. As can be seen in Table 1, the T_m values of chimera AMOs, which contain either 2′-F or 2′-F-4′-thioribonucleoside modification, were higher than those of the uniformly modified AMOs. Although AM21SMF2 showed the highest T_m value, its anti-miR-21 activity was lowest among 4′-thio–modified AMOs. A similar trend was observed in a series of AMOs consisting of 4′-oxo congeners. Thus, no correlation was observed between activity and binding affinity in our case. Meanwhile, as we reported previously (21), 2′-OMe-4′-thioRNA showed higher nuclease stability compared with 2′-OMe RNA, 2′-F-4′-thioRNA and 2′-F RNA. Therefore, chimera AMOs might be more susceptible to degradation than the uniformly modified AMOs, serving as a potential explanation why AM21SM showed the highest activity amongst all AMOs tested. From these results, it can be concluded that the 2′-OMe-4′-thioribonucleoside modification is useful for inhibition of miRNA function. Also, uniform modification is simple and seems to be the most promising choice for subsequent studies.

Improvement in duration of anti-miRNA activity of AMOs by backbone substitution

To examine if 2′-OMe-4′-thioribonucleoside–modified AMO is capable of inhibiting other miRNAs, we chose miR-122 as another miRNA target. MiR-122 is a liver-specific miRNA, known to be involved in cholesterol metabolism, fatty acid metabolism (36) and hepatitis C virus replication (37). Many successful studies of miR-122 inhibition by AMOs both *in vitro* and *in vivo* have been reported (20,36–42), and some of them are currently under investigation in clinical trials (20). We hypothesized that 2′-OMe-4′-thioribonucleoside–modified AMO could have high potency to inhibit miR-122 as well as miR-21.

We synthesized a uniformly 2′-OMe-4′-thioribonucleoside–modified AMO, which is complementary to and the same length (23-mer) as mature miR-122,

Table 2. Sequence and modification pattern of anti-miR-122 AMOs

AMO	Sequence[a]	T_m (°C)[b]
AM122SM	5′-**ACAAACACCAUUGUCACACUCCA**-3′	65.8
AM122SM-PS	5′-**ACAAACACCAUUGUCACACUCCA**-3′	64.8
AM122SM-PS 20 nt	5′-**AAACACCAUUGUCACACUCC**-3′	60.7
AM122SM-PS 15 nt	5′-**CCAUUGUCACACUCC**-3′	54.6
AM122SM-PS 8 nt	5′-**CACACUCC**-3′	36.3
AM122M	5′-ACAAACACCAUUGUCACACUCCA-3′	62.9
AM122M-PS	5′-ACAAACACCAUUGUCACACUCCA-3′	58.0

[a]Upper case letters represent 2′-OMe; bold upper case letters are 2′-OMe-4′-thioribonucleotides; underlined are PS backbone modification., [b]T_ms were measured versus miR-122 in a phosphate buffer (10 mM, pH 7.0) containing 0.1 mM EDTA and 1 mM NaCl, 3 μM strand concentration. Values were given as an average of three independent experiments.

with unmodified phosphodiester (PO) backbone (AM122SM, Table 2). Because ONs can be degraded by nuclease by cleaving a phosphodiester linkage in biological fluid, substitution of a PO linkage for a PS linkage is ideal to prevent such nuclease cleavage reactions. In fact, PS modification has successfully been applied to many previously reported AMOs. Because our end goal of this study is *in vivo* application, we synthesized 2′-OMe-thioribonucleoside–modified AMOs with PS backbones (AM122SM-PS). For comparison, we also synthesized uniformly 2′-OMe–modified AMOs with either PO or PS backbones (AM122M and AM122M-PS, respectively). Recently, Obad *et al.* developed seed targeting 8-mer tiny LNAs, which can simultaneously inhibit miRNA families that share the same seed region (42). According to this report, we also prepared a seed targeting 8-mer (AM122SM-PS 8 nt) along with two shorter sequences (AM122SM-PS 15 nt and AM122SM-PS 20 nt) to examine their potency as well as to find an optimal length of AMOs.

Each AMO and a miR-122 reporter plasmid (pmirGLO 122), constructed in a same manner to pmirGLO21, were co-transfected into Huh-7 cells at various AMO concentrations (0.5–5 nM). At 24 h after transfection, we harvested the cells and carried out dual luciferase reporter assay. The resulting AMO activities were shown in Figure 3. As was the case of miR-21 inhibition, all AMOs showed miR-122 inhibitory activity in a dose-dependent manner, and AM122SM gave higher activity than AM122M (63.9 versus 36.6% at 5 nM). No obvious difference was observed in the activity between AMOs with PO and PS backbones. Concerning of the length of AMO, anti-miRNA activity decreased as AMO length became shorter, and tiny AMO, namely AM122SM PS 8 nt, did not show any activity. Thus, the 2′-OMe-4′-thioribonucleoside–modified AMO possessing complementary matched sequence and length seems to be suitable for miRNA inhibition.

In our previous study, we showed prolonged activity of 2′-OMe-4′-thioribonucleoside–modified siRNA (29). Thus, we expected that the 2′-OMe-4′-thioribonucleoside modification can prolong the activity of AMOs. We next performed a time-course experiment. As described above, no difference between PO and PS AMOs was observed in the activity after 24 h. However, considerable differences

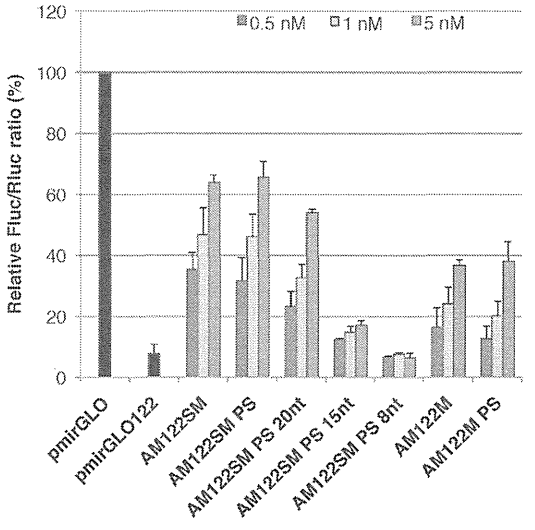

Figure 3. Anti-miR-122 activity of the modified AMOs. Huh-7 cells were co-transfected with the miR-122 reporter plasmid (mirGLO122) and the anti-miR-122 AMOs at the indicated concentrations. The dual luciferase assay was performed at 24 h after transfection. Data are shown as mean with SD.

were observed after 48 h, where the activities of PO AMOs (AM122SM and AM122M) declined (Figure 4), while activities of PS AMOs (AM122SM-PS and AM122M-PS) increased. AM122SM-PS showed dramatic increase of the activity throughout the assay, as much as 90% at 72 h. From these results, it can be concluded that 2′-OMe-4′-thioribonucleoside–modified AMO are superior compared with 2′-OMe–modified AMO, and that PS modification conferred long-term activity on AM122SM.

In the case of the miR-21 study described above, we suggested that nuclease resistance is more closely related to AMO potency than the T_m values. We wished to explore further which of these two factors correlated more strongly with the potency. To explore a correlation between the potency and physical properties of 2′-OMe-4′-thioribonucleotide–modified miR-122 AMOs in more detail, we first measured the T_m values of duplexes with a target miR-122. As can be seen in Table 2, AM122M

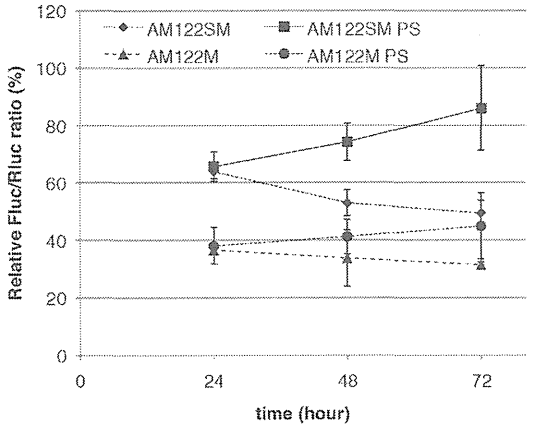

Figure 4. Duration of inhibition by anti-miR-122 AMOs. Huh-7 cells were co-transfected with the miR-122 reporter plasmid (mirGLO122) and the anti-miR-122 AMOs at 5 nM. The dual luciferase assay was performed at the indicated hours. Data are shown as mean with SD.

had a T_m value of 62.9°C and that of AM122M-PS was lower (T_m = 58.0°C and ΔT_m = 4.9°C). On the other hand, AM122SM showed a higher T_m value (65.8°C) compared with that of AM122M, and AM122SM-PS had the T_m value of 64.8°C with only a slight decrease from that of AM122SM (ΔT_m = 1.0°C). It is well known that the PS modification lowers the T_m of ONs (~0.5–0.7°C per modification) (43,44). This decrease of the binding affinity would cause loss of inhibitory activity of AMOs. However, replacement of the PO backbone of AM122SM with a PS had no effect on the binding affinity of the AMO, a possible explanation for the retained AMO activity.

We then investigated the nuclease stability of the modified AMOs. A series of AMOs were labeled at the 5′-end with ^{32}P and incubated in 50% human plasma. The reactions were analyzed by denaturing PAGE (Supplementary Figure S1). As expected, PS AMOs exhibited higher stability than that of PO AMOs, and as we reported previously, 2′-OMe-4′-thioribonucleoside–modified AMOs were slightly more stable than that of the corresponding 2′-OMe–modified AMOs. It is worth noting that AM122SM-PS was totally intact under these conditions, while AM122M-PS showed some mild degradation. The rank order of stability in plasma was AM122SM-PS > AM122M-PS > AM122SM > AM122M, indicating that AM122SM-PS is extremely stable against nuclease degradation in human plasma. These results suggested that the T_m value of the AMO had relatively little impact on AMO potency, whereas nuclease resistance seemed to have much greater effect.

For therapeutic use, nuclease resistance in biological fluid, tissues and cells is a prerequisite feature of chemically modified ONs. Our previous comprehensive study of nuclease stability revealed that 2′-OMe-4′-thioRNA was significantly stable against both exo- and endonucleases in spite of consisting of PO backbones (21). Here, we showed PS modification on the 2′-OMe-4′-thioribonucleoside–modified AMO can further improve its nuclease resistance. As a more specific scenario, the endonuclease activity of Ago2 cleaves the unselected strand of RNA duplexes loading into the RISC. It is thought that AMOs act primarily by hybridizing with mature miRNAs that have been loaded into the RISC. Wang *et al.* explained the molecular mechanisms of target RNA cleavage by a crystal structure of Ago protein (45). They found that both 2′-OMe and PS substitution at the cleavage site (positions 10′–11′) disrupted Ago slicer activity, owing to configurations of the sulfur atoms in Ago protein. Thus, we suggest that the potency and long-term activity of the AM122SM-PS would be due in part to its resistance to cleavage by Ago. Also, PS modification could increase intracellular stability of AMOs, consequently anti-miRNA activity AMOs increased over time (Figure 4). Taken together, combinatorial use of 2′-OMe-4′-thioribonucleosides and a PS backbone is an attractive choice for therapeutic AMOs.

Targeted delivery and anti-miR-122 activity of 2′-OMe-4-thioribonucleoside–modified AMO in mouse liver

In vitro studies showed that AM122SM-PS possessed the most favorable properties. Hence, we next carried out *in vivo* studies to assess whether AM122SM-PS could also inhibit miR-122 in mice.

Two aspects of successful nucleic acid therapeutics are delivery, followed by ON stability. We have developed a new liposomal nucleic acid delivery system, YSK05-MEND, which contains a pH-sensitive cationic lipid for efficient release of siRNAs from the endosome into the cytoplasm (29). Thus, we prepared YSK05-MEND for *in vivo* delivery of AMOs to the liver. YSK05-MENDs encapsulating AM122M-PS and AM122SM-PS represented comparable size, charge, polydispersity and encapsulation efficiency (Supplementary Table S2). We assessed *in vivo* efficacy of the modified miR-122 AMOs by treating mice three times with intravenous injection of 1 mg/kg YSK05-MEND formulated AMO122SM-PS or AMO122M-PS every 2 days.

As described above, a single miRNA may control the levels of multiple mRNAs (3–6). MiR-122 is no exception, as many mRNAs whose expressions are directly controlled by miR-122 have been identified. Elmén *et al.* demonstrated inhibition of miR-122 using LNA-modified AMOs, LNA-antimiR (41). In their experiments, derepressions of four mRNAs, AldoA, Bckdk, Ndrg3 and Cd320, all of which are direct targets of miR-122 in the mouse liver, were observed after treatment of mice with LNA-antimiR. Therefore, we conducted expression analysis of three miR-122 target mRNAs in the mouse liver, AldoA, Bckdk and Ndrg3 (Figure 5A), by real-time PCR 48 h after the last injection. The levels of all three mRNAs were higher in the AMO-treated mice compared with those treated with saline. It is worth noting that AM122SM-PS induced higher mRNA expression levels than AM122M-PS in all three mRNAs examined. We also observed statistically significant differences between AM122SM-PS and AM122M-PS in the expressions of both AldoA and Bckdk ($P < 0.05$).

We next examined the change in plasma cholesterol level associated with the increase in expression of these

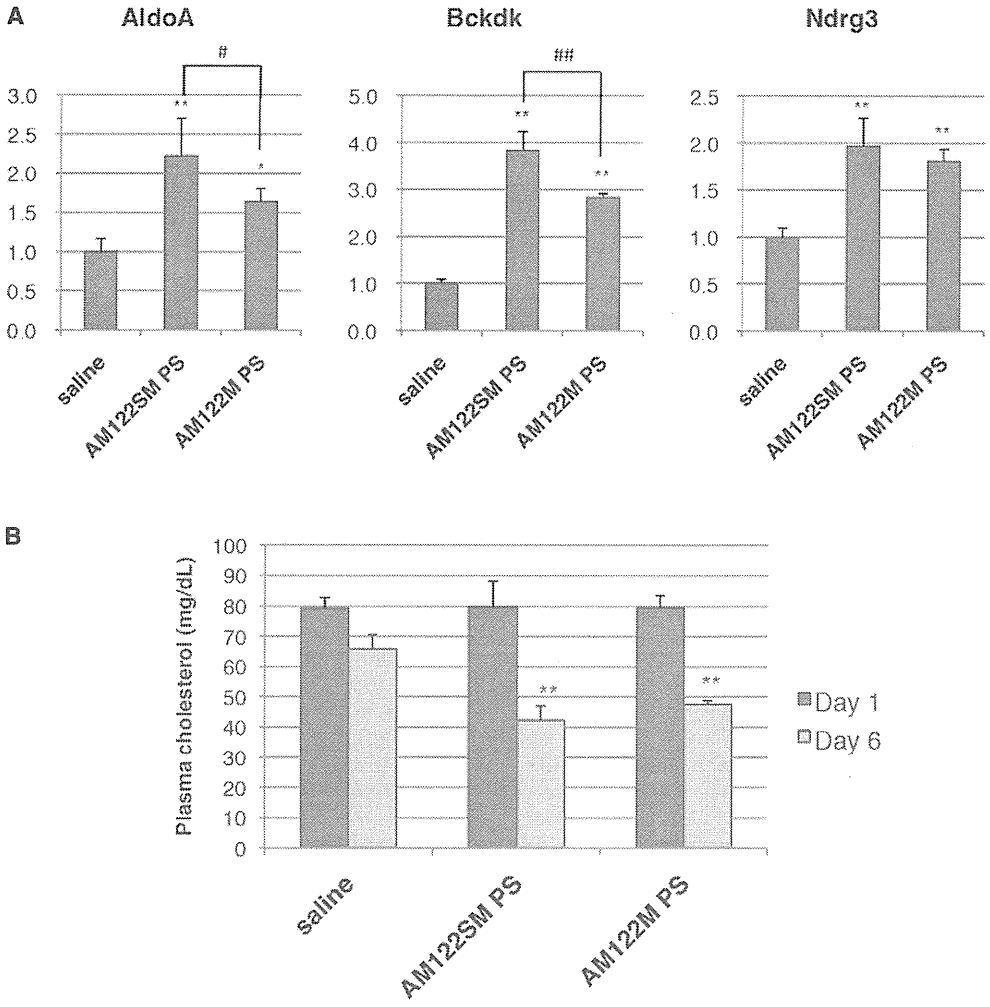

Figure 5. Inhibition of miR-122 in mice. (**A**) Levels of miR-122 target genes in liver RNA analyzed by qRT-PCR. Each mRNA level was normalized to the mean of saline control group. Data are shown as mean with SD ($n = 4$, 48 h). (**B**) Plasma cholesterol levels in mice. The data were normalized to the mean of saline control group at each time point (Day 1 and Day 6). Data are shown as mean with SD ($n = 4$). $^{*}P < 0.05$, $^{**}P < 0.01$ versus saline, $^{\#}P < 0.05$, $^{\#\#}P < 0.01$ determined by one-way ANOVA followed by SNK test.

mRNAs. There was no obvious difference between the AMO- and saline-treated mice at 1 day after the last dose, while drastic changes were observed at day 6, where the serum cholesterol levels were reduced by 57.7% for AM122SM-PS and 52.5% for AM122M-PS (Figure 5B) without any hepatotoxicity (Supplementary Figure S2). These results suggest that AM122SM-PS was properly delivered to the mouse liver by YSK05-MEND and elicited an anti-miR-122 effect.

In the previous reports (20,36–38,40–42), AMOs have been administered either as naked/saline formulated or as small molecule conjugates (e.g. cholesterol, a cell-penetrating peptide) to assist *in vivo* delivery. These approaches often required relatively high doses (ranging from 10 to 80 mg/kg for mice). Instead, our YSK05-MEND dosing strategy achieves efficient miR-122 AMO delivery to the liver. Although the mouse strains used for our experiments versus other researchers' previous studies were different (e.g. we used inbred strain mice, BALB/c, which are considered to be genetically identical, whereas others used outbred strains, such as NMRI), we successfully increased miR-122 target mRNA expression, followed by a decrease in serum cholesterol level with three intravenous doses of 1 mg/kg AM122SM-PS in mice.

CONCLUSION

We demonstrated the inhibition of miRNAs with 2′-OMe-4′-thioribonucleoside–modified AMOs *in vitro* as well as *in vivo*. We first evaluated a variety of chemically modified AMOs that are complementary to mature miR-21, and found the potency of the uniformly 2′-OMe-4′-thioribonucleoside–modified AMO to be the

best in our series. Further investigation revealed that PS modification contributes to long-term miR-122 inhibition by the 2′-OMe-4′-thioribonucleoside–modified AMO.

For *in vivo* studies, we took advantage of an efficient delivery technology, YSK05-MEND, and successfully increased three miR-122 target mRNA levels in the AMO-treated mice liver, followed by a decline of serum cholesterol levels. Although many successful *in vivo* AMO studies have been reported so far, to our knowledge, none of them have used liposome-like delivery systems. In our previous study, we confirmed that YSK05-MEND efficiently releases siRNAs into the cytoplasm in a pH-dependent manner (30). It is with this property that we believe we were able to achieve efficient AMO delivery in mice.

Together, here we showed not only the potency of 2′-OMe-4′-thioribonucleoside–modified AMOs but also the utility of YSK05-MEND for AMO delivery. Further *in vivo* studies leading to the understanding of the mechanism of the 2′-OMe-4′-thioribonucleoside–modified AMO function as well as their potential side effect are currently under way.

SUPPLEMENTARY DATA

Supplementary Data are available at NAR Online.

ACKNOWLEDGEMENT

The authors would like to thank Ms Y. Misawa (Hokkaido University) for technical assistance.

FUNDING

Grant-in-Aid for Scientific Research [23249008]; Grant-in-Aid for Scientific Research on Innovative Area "Nanomedicine Molecular Science" [2306] from the Ministry of Education, Culture, Sports, Science and Technology in Japan. Funding for open access: Grant-in-Aid for Scientific Research [23249008].

Conflict of interest statement. None declared.

REFERENCES

1. Liu,Z., Sall,A. and Yang,D. (2008) MicroRNA: an emerging therapeutic target and intervention. *Int. J. Mol. Sci.*, **9**, 978–999.
2. Krol,J., Loedige,I. and Filipowicz,W. (2010) The widespread regulation of microRNA biogenesis, function and decay. *Nat. Rev. Genet.*, **11**, 597–610.
3. Lewis,B., Shih,I., Jones-Rhoades,M., Bartel,D. and Burge,C. (2003) Prediction of mammalian microRNA targets. *Cell*, **115**, 787–798.
4. Krek,D., Grün,D., Poy,M.N., Wolf,R., Rosenberg,L., Epstein,E.J., MacMenamin,P., da Piedade,I., Gunsalus,K.C., Stoffel,M. *et al.* (2005) Combinatorial microRNA target predictions. *Nat. Genet.*, **37**, 495–500.
5. Betel,D., Wilson,M., Gabow,A., Marks,D.S. and Sander,C. (2008) The microRNA.org resource: targets and expression. *Nucleic Acids Res.*, **36**, D149–D153.
6. Friedman,R.C., Farh,K.K., Burge,C.B. and Bartel,D.P. (2009) Most mammalian mRNAs are conserved targets of microRNAs. *Genome Res.*, **19**, 92–105.
7. Lewis,B.P., Burge,C.B. and Bartel,D.P. (2005) Conserved seed pairing, often flanked by adenosines, indicates that thousands of human genes are microRNA targets. *Cell*, **120**, 15–20.
8. Sayed,D. and Abdellatif,M. (2011) MicroRNAs in development and disease. *Physiol. Rev.*, **91**, 827–887.
9. Esau,C.C. (2008) Inhibition of microRNA with antisense oligonucleotides. *Methods*, **44**, 55–60.
10. Inoue,H., Hayase,Y., Iwai,S. and Ohtsuka,E. (1987) Sequence-dependent hydrolysis of RNA using modified oligonucleotide splints and RNase H. *FEBS Lett.*, **215**, 327–330.
11. Inoue,H., Hayase,Y., Imura,A., Iwai,S., Miura,K. and Ohtsuka,E. (1987) Sythesis and hybridization studies on two complementary nona(2′-*O*-methyl)ribonucleotides. *Nucleic Acids Res.*, **15**, 6131–6148.
12. Lesnik,E.A., Guinosso,C.J., Kawasaki,A.M., Sasmor,H., Zounes,M., Cummins,L.L., Ecker,D.J., Cook,P.D. and Freier,S.M. (1993) Oligodeoxynucleotides containing 2′-O-modifies adenosine: synthesis and effects on stability of DNA: RNA duplexes. *Biochemistry*, **32**, 7832–7838.
13. Cummins,L.L., Owens,S.R., Risen,L.M., Lesnik,E.A., Freier,S.M., McGee,D., Guinosso,C.J. and Cook,P.D. (1995) Characterization of fully 2′-modified oligonucleotide hetero- and homoduplex hybridization and nuclease sensitivity. *Nucleic Acids Res.*, **23**, 2019–2024.
14. Teplova,M., Minasov,G., Tereshko,V., Inamati,G.B., Cook,P.D., Manoharan,M. and Egli,M. (1999) Crystal structure and improved antisense properties of 2′-*O*-(2-methoxyethyl)-RNA. *Nat. Struct. Biol.*, **6**, 535–539.
15. Obika,S., Nanbu,D., Hari,Y., Morio,K., In,Y., Ishida,T. and Imanishi,T. (1997) Synthesis of 2′-*O*,4′-*C*-methyleneuridine and-cytidine: novel bicyclic nucleosides having a fixed C3′-endo sugar puckering. *Tetrahedron Lett.*, **38**, 8735–8738.
16. Christensen,N.K., Petersen,M., Nielsen,P., Jacobsen,J.P., Olsen,C.E. and Wengel,J. (1998) A novel class of oligonucleotide analogues containing 2′-*O*,3′-*C*-linked [3.2.0]bicycloarabinonucleoside monomers: synthesis, thermal affinity studies, and molecular modeling. *J. Am. Chem. Soc.*, **120**, 5458–5463.
17. Bennett,C.F. and Swayze,E.E. (2010) RNA targeting therapeutics: molecular mechanisms of antisense oligonucleotides as a therapeutic platform. *Annu. Rev. Pharmacol. Toxicol.*, **50**, 259–293.
18. Meister,G., Landthaler,M., Dorsett,Y. and Tuschl,T. (2004) Sequence-specific inhibition of micro-RNA- and siRNA-induced RNA silencing. *RNA*, **10**, 544–550.
19. Hutvagner,G., Simard,M.J., Mello,C.C. and Zamore,P.D. (2004) Sequence-specific inhibition of small RNA function. *PLoS Biol.*, **2**, E98.
20. Lanford,R.E., Hildebrandt-Eriksen,E.S., Petri,A., Persson,R., Lindow,M., Munk,M.E., Kauppinen,S. and Ørum,H. (2010) Therapeutic silencing of microRNA-122 in primates with chronic hepatitis C virus infection. *Science*, **327**, 198–201.
21. Takahashi,M., Minakawa,N. and Matsuda,A. (2009) Synthesis and characterization of 2′-modified-4′-thioRNA: a comprehensive comparison of nuclease stability. *Nucleic Acids Res.*, **37**, 1353–1362.
22. Naka,T., Minakawa,N., Abe,H., Kaga,D. and Matsuda,A. (2000) The stereoselective synthesis of 4′-β-thioribonucleosides via the Pummerer reaction. *J. Am. Chem. Soc.*, **122**, 7233–7243.
23. Hoshika,S., Minakawa,N. and Matsuda,A. (2004) Synthesis and physical and physiological properties of 4′-thioRNA: application to post-modification of RNA aptamer toward NF-κB. *Nucleic Acids Res.*, **32**, 3815–3825.
24. Hoshika,S., Minakawa,N., Kamiya,H., Harashima,H. and Matsuda,A. (2005) RNA interference induced by siRNAs modified with 4′-thioribonucleosides in cultured mammalian cells. *FEBS Lett.*, **579**, 3115–3118.
25. Hoshika,S., Minakawa,N., Shionoya,A., Imada,K., Ogawa,N. and Matsuda,A. (2007) Study of modification pattern–RNAi activity relationships by using siRNAs modified with 4′-thioribonucleosides. *Chembiochem.*, **8**, 2133–2138.
26. Kato,Y., Minakawa,N., Komatsu,Y., Kamiya,H., Ogawa,N., Harashima,H. and Matsuda,A. (2005) New NTP analogs: the synthesis of 4′-thioUTP and 4′-thioCTP and their utility for SELEX. *Nucleic Acids Res.*, **33**, 2942–2951.

27. Minakawa,N., Sanji,M., Kato,Y. and Matsuda,A. (2008) Investigations toward the selection of fully-modified 4′-thioRNA aptamers: optimization of *in vitro* transcription steps in the presence of 4′-thioNTPs. *Bioorg. Med. Chem.*, **16**, 9450–9456.
28. Dande,P., Prakash,T.P., Sioufi,N., Gaus,H., Jarres,R., Berdeja,A., Swayze,E.E., Griffey,R.H. and Bhat,B. (2006) Improving RNA interference in mammalian cells by 4′-thio-modified small interfering RNA (siRNA): effect on siRNA activity and nuclease stability when used in combination with 2′-*O*-alkyl modifications. *J. Med. Chem.*, **49**, 1624–1634.
29. Takahashi,M., Nagai,C., Hatakeyama,H., Minakawa,N., Harashima,H. and Matsuda,A. (2012) Intracellular stability of 2′-OMe-4′-thioribonucleoside modified siRNA leads to long-term RNAi effect. *Nucleic Acids Res.*, **40**, 5787–5793.
30. Sato,Y., Hatakeyama,H., Sakurai,Y., Hyodo,M., Akita,H. and Harashima,H. (2012) A pH-sensitive cationic lipid facilitates the delivery of liposomal siRNA and gene silencing activity *in vitro* and *in vivo*. *J. Control. Release*, **163**, 267–276.
31. Sakurai,Y., Hatakeyama,H., Sato,Y., Hyodo,M., Akita,H. and Harashima,H. (2013) Gene silencing via RNAi and siRNA quantification in tumor tissue using MEND, a liposomal siRNA delivery system. *Mol. Ther.*, **21**, 1195–1203.
32. Krichevsky,A.M. and Gabriely,G. (2009) miR-21: a small multi-faceted RNA.J. *Cell. Mol. Med.*, **13**, 39–53.
33. Takahashi,M., Daidouji,S., Shiro,M., Minakawa,N. and Matsuda,A. (2008) Synthesis and crystal structure of 2′-deoxy-2′-fluoro-4′-thioribonucleosides: substrates for the synthesis of novel modified RNAs. *Tetrahedron*, **64**, 4313–4324.
34. Horwich,M. and Zamore,P. (2008) Design and delivery of antisense oligonucleotides to block microRNA function in cultured *Drosophila* and human cells. *Nat. Protoc.*, **3**, 1537–1549.
35. Lennox,K.A. and Behlke,M.A. (2010) A direct comparison of anti-microRNA oligonucleotide potency. *Pharm. Res.*, **9**, 1788–99.
36. Esau,C., Davis,S., Murray,S.F., Yu,X.X., Pandey,S.K., Pear,M., Watts,L., Booten,S.L., Graham,M., McKay,R. *et al.* (2006) miR-122 regulation of lipid metabolism revealed by in vivo antisense targeting. *Cell Metab.*, **3**, 87–98.
37. Jopling,C.L., Yi,M., Lancaster,A.M., Lemon,S.M. and Sarnow,P. (2005) Modulation of hepatitis C virus RNA abundance by a liver-specific microRNA. *Science*, **309**, 1577–1581.
38. Krützfeldt,J., Rajewsky,N., Braich,R., Rajeev,K.G., Tuschl,T., Manoharan,M. and Stoffel,M. (2005) Silencing of microRNAs *in vivo* with 'antagomirs'. *Nature*, **438**, 685–689.
39. Davis,S., Lollo,B., Freier,S. and Esau,C. (2006) Improved targeting of miRNA with antisense oligonucleotides. *Nucleic Acids Res.*, **34**, 2294–2304.
40. Davis,S., Propp,S., Freier,S.M., Jones,L.E., Serra,M.J., Kinberger,G., Bhat,B., Swayze,E.E., Bennett,C.F. and Esau,C. (2009) Potent inhibition of microRNA *in vivo* without degradation. *Nucleic Acids Res.*, **37**, 70–77.
41. Elmén,J., Lindow,M., Silahtaroglu,A., Bak,M., Christensen,M., Lind-Thomsen,A., Hedtjärn,M., Hansen,J.B., Hansen,H.F., Straarup,E.M. *et al.* (2008) Antagonism of microRNA-122 in mice by systemically administered LNA-antimiR leads to up-regulation of a large set of predicted target mRNAs in the liver. *Nucleic Acids Res.*, **36**, 1153–1162.
42. Obad,S., dos Santos,C.O., Petri,A., Heidenblad,M., Broom,O., Ruse,C., Fu,C., Lindow,M., Stenvang,J., Straarup,E.M. *et al.* (2011) Silencing of microRNA families by seed-targeting tiny LNAs. *Nat. Genet.*, **43**, 371–378.
43. Freier,S.M. and Altmann,K.H. (1997) The ups and downs of nucleic acid duplex stability: structure-stability studies on chemically-modified DNA: RNA duplexes. *Nucleic Acids Res.*, **25**, 4429–4443.
44. Stein,C.A., Subasinghe,C., Shinozuka,K. and Cohen,J.S. (1988) Physicochemical properties of phosphorothioate oligodeoxynucleotides. *Nucleic Acids Res.*, **16**, 3209–3221.
45. Wang,Y., Juranek,S., Li,H., Sheng,G., Wardle,G.S., Tuschl,T. and Patel,D.J. (2009) Nucleation, propagation and cleavage of target RNAs in Ago silencing complexes. *Nature*, **461**, 754–761.

Gene Silencing via RNAi and siRNA Quantification in Tumor Tissue Using MEND, a Liposomal siRNA Delivery System

Yu Sakurai[1], Hiroto Hatakeyama[1], Yusuke Sato[1], Mamoru Hyodo[1], Hidetaka Akita[1] and Hideyoshi Harashima[1]

[1]*Faculty of Pharmaceutical Sciences, Hokkaido University, Sapporo, Japan*

Small interfering RNA (siRNA) would be predicted to function as a cancer drug, but an efficient siRNA delivery system is required for clinical development. To address this issue, we developed a liposomal siRNA carrier, a multifunctional envelope-type nanodevice (MEND). We previously reported that a MEND composed of a pH-sensitive cationic lipid, YSK05, showed significant knockdown in both *in vitro* and in tumor tissue by intratumoral injection. Here, we report on the development of an *in vivo* siRNA delivery system that is delivered by systemic injection and an analysis of the pharmacokinetics of an intravenously administered siRNA molecule in tumor tissue. Tumor delivery of siRNA was quantified by means of stem-loop primer quantitative reverse transcriptase PCR (qRT-PCR) method. PEGylation of the YSK-MEND results in the increase in the accumulation of siRNA in tumor tissue from 0.0079% ID/g tumor to 1.9% ID/g tumor. The Administration of the MEND (3 mg siRNA/kg body weight) showed about a 50% reduction in the target gene mRNA and protein. Moreover, we verified the induction of RNA interference by 5′ RACE-PCR method. The collective results reported here indicate that an siRNA carrier was developed that can deliver siRNA to a target cell in tumor tissue through an improved siRNA bioavailability.

Received 22 November 2012; accepted 5 March 2013; advance online publication 9 April 2013. doi:10.1038/mt.2013.57

INTRODUCTION

A small interfering RNA (siRNA) is thought to be a new class of medicines for cancer treatment because siRNA can, in principle, inhibit the expression of any genes of interest.[1,2] However, naked siRNA is easily degraded in the blood stream by ribonuclease and cannot pass through a cellular membrane because of its large molecular size and high hydrophilicity. These properties clearly suggest that an efficient delivery system for siRNA that specifically targets cancer cells is required for developing an RNAi medicine.[3] Many groups have reported on the development of siRNA delivery system for tumor targeting using a variety of formulations, such as polyplexes, lipoplexes, micelles, and liposomes.[4] To address this issue, we developed a multifunctional envelope-type nanodevice (MEND) containing macromolecules such as oligonucleotides and proteins in free forms or condensed forms with a polycation that are encapsulated within a lipid envelope.[5]

Macromolecules that have a prolonged retention time in the blood stream can passively accumulate in tumor tissue. The passive accumulation in the tumor results from its abnormal vasculature, namely an aberrant vascular architecture and lack of lymphatic drainage, which is referred to as the enhanced permeability and retention (EPR) effect.[6] Generally, materials that are delivered are highly positive charged that permits them to electrostatically interact with the negatively charged siRNA. Although attempts have been made to use the EPR effect to deliver siRNA to tumor tissue in many siRNA delivery systems, the highly positively charged carriers are rapidly eliminated from the circulation, which results in a poor EPR effect.[7] This is because a positively charged material is immediately recognized by serum proteins and immune cells in the blood.[3] Therefore, carriers with a high cationic charge must be coated with a large amount of polyethylene glycol (PEG) to prevent their recognition by immune cells or serum proteins in the blood stream. Modifying an siRNA carrier with a heavy coating of PEG results in a low cellular uptake and attenuated endosomal escape, and hence, a decrease in siRNA delivery ability.[8] We have attempted to overcome this discrepancy by using cleavable PEG in response to an enzyme that is highly expressed in cancer cells and a pH-sensitive fusogenic peptide, and found that these systems could induce gene silencing in tumor tissue.[9,10] These systems circumvented the issue by removing PEG or assisting endosomal escape with the peptide. However, as these carriers were composed of a conventional cationic lipid, 1,2-dioleoyltrimethylammoniumpropane (DOTAP), a 10–15 mol% of PEG modification to mask the positively charged surface of the MEND was needed for a prolonged circulation. To avoid such an extensive PEG modification, we recently approached this dilemma by designing a new pH-sensitive cationic lipid, YSK05.[11] We reported that YSK05 had a high pH-responsive fusogenic ability derived from the unique head group and fatty acid in the preparation. A MEND that contained YSK05 has a higher gene-knockdown ability than the commercially available transfection reagent (Lipofectamine 2000) and demonstrated a significant gene reduction by intratumoral injection in tumor-bearing mice. We

Correspondence: *Hideyoshi Harashima, Kita-12, Nishi-6, Kita-ku, Sapporo 060-0812, Japan. E-mail: harasima@pharm.hokudai.ac.jp*

also already clarified that a MEND composed of YSK05 required a relatively small amount of PEG modification to confer adequate pharmacokinetics characteristics, because YSK05 was neutral in the blood because of its appropriate pKa. This result suggests that a MEND composed of YSK05 would be suitable for delivering siRNA to tumor tissue. In this study, we first attempted to identify an appropriate lipid composition for the *in vivo* circumstance with liver as a model organ. We then used the post-PEGylated YSK05-MEND for targeting cancer, aimed at the gene-silencing effect in tumor tissue via its systemic administration.

To develop a more efficient siRNA carrier, it is important to analyze the biodistribution of siRNA after systemic injection and to determine the precise mechanism responsible for gene reduction. A well-validated method for quantifying the amount of siRNA in blood or in organs was recently reported.[12] In the report, the amount of siRNA, even if chemically modified or formulated into a lipid nanoparticle, in the mouse liver after systemic injection could be measured with high sensitivity and selectivity. We applied this method in this study for the quantification of siRNA in subcutaneously inoculated tumor tissue and evaluated the effect on the efficiency of siRNA delivery. In addition, the off-target effect of siRNA can lead to artificial phenotypes and a complicated understanding of the therapeutic effects of siRNA. The causes of off-target effects can be roughly classified into three types: microRNA-like effect, immunostimulatory effect via toll-like receptors (TLRs), and competition with the RNAi machinery with endogenous microRNAs.[13] For example, the immune stimulation effect of siRNA can show a therapeutic effect via the production of inflammatory cytokines by inhibiting neovascularization.[14] Therefore, for development of an siRNA medicine, it is necessary to distinguish between siRNA-induced gene silencing from non-specific effects. We herein report that a MEND composed of our unique cationic lipid, YSK05, can induce gene silencing via RNAi.

RESULTS

Construction of the YSK05-MEND

As we previously reported on the optimized lipid composition of the YSK05-MEND (please refer to **Supplementary Figure S1** on the structural information of YSK05) was YSK05/POPE/chol/$PEG_{2,000}$-DMG=50/25/25/3 (POPE; 1-palmitoyl-2-oleoyl-sn-glycero-3-phosphoethanolamine, $PEG_{2,000}$-DMG; 1,2-dimyristoyl-sn-glycerol, PEG) for *in vitro* transfection activity,[11] we first investigated the issue of whether the optimized MEND resulted in a reduction in the target gene in the liver, using the scavenger receptor B1 (*Srb1*) as a target gene. The liver, in which liposomal carriers tended to accumulate, was used as a model organ for a verification of the *in vivo* potential of the MEND containing YSK05 for the sake of simplicity. However, the MEND containing POPE, as a helper lipid, failed to silence *SrbI* mRNA (**Supplementary Figure S2a**). We next tested the gene-silencing effect of the POPE-based MEND in tumor tissue after systemic injection. We chose polo-like kinase 1 (*PLK1*) as an anticancer gene, because it has been validated as a well-known target for cancer therapy.[15] When PEGylation was performed by coincubating micelles of $PEG_{2,000}$-DSG ($PEG_{2,000}$-DSG; 1,2-distearoyl-sn-glycerol, PEG) with the MEND at 45 °C for 45 minutes in a 10% ethanol solution for using the EPR effect, the post-PEGylated POPE-based MEND also showed no silencing effect in tumor tissue (**Supplementary Figure S2b**). Phosphoethanolamine was judged to be the inappropriate head group of the helper lipid, as previous reports showed that the phosphoethanolamine head group was more readily recognized by immune cells rather than hepatocytes[16] Accordingly, we replaced POPE with 1,2-distearoyl-sn-glycero-3-phosphocholine (DSPC) and improved the lipid ratio in accordance with findings reported from other investigators.[17] As a result, in the liver, DSPC-based MEND showed a significant knockdown (**Supplementary Figure S2a**). In summary, the basal lipid composition for *in vivo* applications was determined to be YSK05/cholesterol/DSPC/$PEG_{2,000}$-DMG at a ratio of 50/40/10/3.

Table 1 Characteristics of the MENDs

	MEND	PEG-MEND
	YSK05/DSPC/ chol/$PEG_{2,000}$-DMG	YSK05/DSPC/ chol/$PEG_{2,000}$-DMG/ $PEG_{2,000}$-DSG
Lipid	**50/10/40/3**	**50/10/40/3/5**
z-average (nm)	104 ± 6	101 ± 8
Polydispersity index	0.16 ± 0.02	0.18 ± 0.03
ζ-potential (mV)	3.3 ± 1.5	2.6 ± 2.0

Data are represented by mean ± SD.

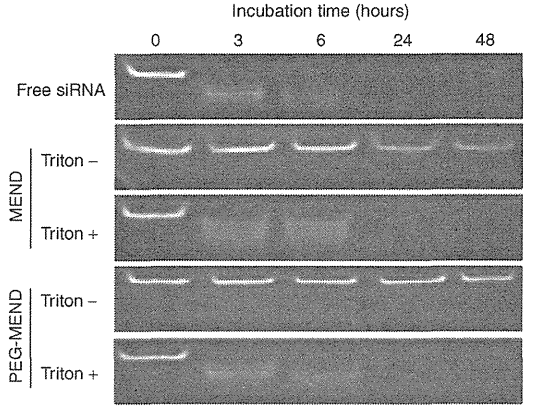

Figure 1 Stability of siRNA encapsulated into MENDs in mouse serum. Naked and formulated siRNAs were coincubated with mouse serum for 48 hours, and then analyzed the integrity of siRNA by TBE-PAGE. MEND, multifunctional envelope-type nanodevice.

As plasma a concentration of >5 mol% of PEGylation on the surface of MEND was saturated, the amount of PEGylation was determined to be 5 mol% (**Supplementary Figure S3**). The average z-average diameter and ζ-potential of the MENDs are shown in **Table 1**. With (PEG-MEND) or without (MEND) 5 mol% PEG insertion, their z-average diameters were nearly 100 nm and their ζ-potentials were almost neutral. The particle size distributions of both MENDs were homogenous, judged from the polydispersity index (PdI). To investigate whether siRNA was assembled into the lipid envelope, the siRNA encapsulated in MENDs was exposed to 90% mouse serum that contained abundant levels of RNase for periods of up to 48 hours (**Figure 1**). Both MENDs prevented the degradation of the siRNA by RNase in plasma for periods of up to 48 hours. However, in the presence of Triton X-100, the formulated siRNA was as rapidly degraded as free siRNA.

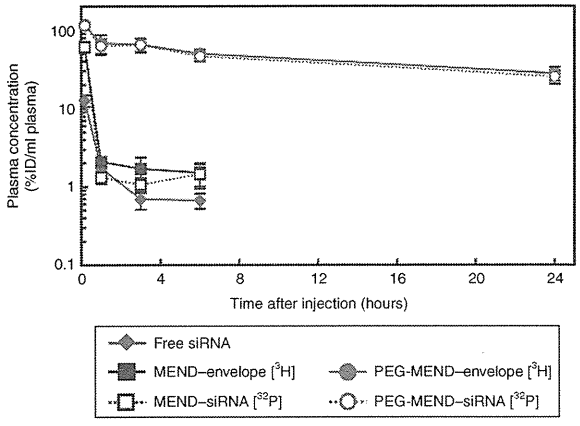

Figure 2 Blood concentration profile of systemically injected MENDs. The lipid envelope and siRNA were labeled with RIs [^{3}H] and [^{32}P], respectively. MENDs and free siRNA were injected via the tail vein of ICR mice, and then at 0.17, 1, 3, 6, and 24 hours after injection, the radio activity in plasma was measured by liquid scintillation counting. The data are represented as the mean ± SD (n = 3). MEND, multifunctional envelope-type nanodevice; RI, radio isotope.

Pharmacokinetics analysis of systemically injected MENDs and free siRNA

We previously reported on a method for evaluating the blood concentrations of both siRNA and a lipid envelope, using two radio isotopes (RIs), [^{3}H] and [^{32}P] as a tracer for the lipid envelope and siRNA, respectively. [^{32}P]-labeled siRNA was synthesized by conjugating 5′ end of siRNA with [^{32}P]-phosphate, as previously reported.[10] In this study, we compared the siRNA concentration in plasma between MEND and PEG-MEND after intravenous injection into normal mice (**Figure 2**). Although the siRNA encapsulated in the MEND was as rapidly eliminated from the blood stream as free siRNA, the siRNA formulated in the PEG-MEND showed a higher blood concentration (30% ID/ml plasma, 24 hours after injection). Moreover, the concentration of the lipid component was equal to that of the siRNA in the PEG-MEND. The half-life in β phase of free siRNA and the siRNA encapsulated in the MEND or PEG-MEND calculated by fitting to a 2-compartment model were 1.5, 1.1, and 16.9 hours, respectively. Additional pharmacokinetics parameters are shown in **Supplementary Table S1**.

Tumor accumulation of encapsulated siRNA and lipid envelope

To measure the amount of siRNA and lipid envelope that was accumulated in tumor tissue, we prepared the tumor-bearing mice by innoculating nude mice with OS-RC-2 cells (renal cell cancer) on the right flank. A higher accumulation of lipid marker (4.0% ID/g tumor) in PEG-MEND was detected than in the MEND (**Figure 3a**). Concerning the siRNA, 3.0% ID/g of tumor and 5.1% ID/g of tumor had accumulated in the case of the MEND and PEG-MEND, respectively (**Supplementary Figure S5**). To verify the high accumulation in the MEND, we attempted to quantify the siRNA accumulation by means of a stem-loop qRT-PCR method. In the case of the PEG-MEND, 1.9% ID/g of tumor of siRNA had accumulated, which was 240-times higher than that for the MEND (**Figure 3b**). To further investigate the distribution of formulated siRNAs, tumor sections after encapsulating fluorescence-labeled siRNA in the MEND were observed by confocal laser scanning microscopy. Numerous red dots, indicative of siRNA, were observed only in the PEG-MEND–treated group (**Figure 3c–e**).

Gene silencing in tumor tissue after the systemic injection of MENDs

We compared the MEND and PEG-MEND with reference to their *in vivo* gene-knockdown effects. Each MEND was injected into the tail veins of OS-RC-2–bearing mice, and the mRNA expression of the target gene was measured by the qRT-PCR method. At a dosage of 4 mg siRNA/kg of body weight, the clear reduction in the target gene was observed only in the case of the PEG-MEND, whereas the MEND failed to suppress *PLK1* mRNA expression (**Figure 4**). Next, a dose-response curve for mRNA expression was constructed (**Figure 5a**). *PLK1* expression was decreased in a dose-dependent manner, and up to 3 mg/kg (a significant gene silencing) was observed, whereas a 5 mg/kg injection of control siRNA (anti-luciferase, si-*luc*) assembled in the PEG-MEND failed to induce any detectable target gene expression. A western blotting analysis revealed that PLK1 protein levels were also suppressed after an anti-*PLK1* siRNA (si-*PLK1*) intravenous administration (**Figure 5b**).

5′ RACE-PCR method for the evaluation of RNAi-induced silencing

To exclude the possibility that the reduction in *PLK1* expression was nonspecific, we carried out the RNA-ligase–mediated rapid amplification of 5′ cDNA ends by the PCR (5′ RACE-PCR) method. In the method, only the mRNA cleaved by siRNA, not uncleaved mRNA, was detected. As shown in **Figure 6a**, nested PCR was performed for a specific and substantial amplification of a small amount of cleaved mRNA fragment. Two sequential PCRs of cleaved mRNA would generate the 307 bp PCR product that exhibits RNAi-induced silencing. Only in the group treated with si-*PLK1*, about a 300 bp fragment was detected (**Figure 6b**). To confirm that the fragment showed the cleaved mRNA, the sequence of the PCR products was determined by DNA sequencing (**Figure 6c**). The predicted sequence was observed in each sample of the si-*PLK1*–treated group.

Toxicological analyses

Finally, we tested the toxicity of the MENDs. As the liver is one of the main clearance organs for liposomes, liver toxicity sometimes becomes a limitation to therapeutic usage. After the intravenous injection of both MENDs, the activities of asparate aminotransferase and alanine aminotransferase, which are typically used as a marker of liver injury, were measured. In all treated groups, no significant change was observed compared with untreated mice at 24 hours after administration (**Figure 7a**). In addition, IL-6 was not produced by the injection of either MEND, whereas poly I:C administration at a dose of 4 mg/kg induced abundant levels of IL-6 (**Figure 7b**). These results suggest that the PEG-MEND shows no acute side effects.

DISCUSSION

As it has been reported that non-specific effects, such as the immune stimulation of injected siRNA, could affect the therapeutic effect,[18]

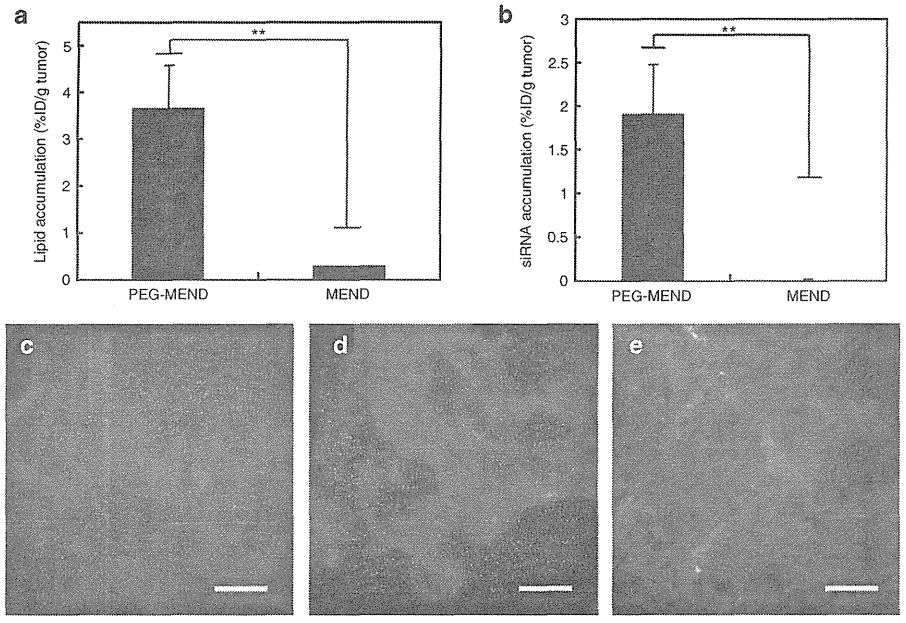

Figure 3 Tumor accumulation of MEND components. (**a**) Lipid envelope accumulation was evaluated by RI. MENDs were labeled with [^{3}H]-cholesteryl-hexadecyl ether (CHE), and then systemically injected into the tail vein of ICR mice. The amount of lipid envelope accumulation was calculated from the count of [^{3}H] in tumor lysate 24 hours after injection. (**b**) siRNA accumulation was determined by the stem-loop qRT-PCR method. The amount of intact siRNA molecules was determined from a standard curve plotted by external siRNA in non-treatment tumor lysate. $^{**}P < 0.01$ (by two-tail unpaired *t*-test). The data are represented as the mean ± SD ($n = 3$). (**c–e**) CLSM observation of tumor tissue. Free and formulated Cy5-labeled siRNA into MENDs were systemically administered into the tumor-bearing mice at a dose of 4 mg/kg, and 6 hours and tumor tissue was collected after the injection. Thick tumor sections of 16 μm were prepared with a cryostat, and tumor sections derived from the mice (**c**) untreated, (c) treated with MEND and (**e**) treated with PEG-MEND were observed by CLSM. Red and green correspond to Cy5-labeled siRNA and fluorescein-isolectin B4 (endothelial cell), respectively. Scale bars: 40 μm. CLSM, confocal laser scanning microscopy; MEND, multifunctional envelope-type nanodevice; PEG, polyethylene glycol; qRT-PCR, quantitative reverse transcriptase PCR; RI, radio isotope.

it is important to confirm RNAi-mediated silencing in the targeted tissue. Hence, we verified whether a MEND composed of a cationic lipid YSK05 could deliver siRNA to tumor tissue and subsequently silence the target gene expression via RNAi machinery.

We attempted to overcome the adverse effect of PEG modification on the ability to deliver siRNA in a subcellular level by using a functional device, such as a PEG-peptide-DOPE (PPD; DOPE, 1,2-dioleoyl-sn-grycelophophoethanolamine) ternary conjugate and a short GALA (shGALA).[9,10,19] In the PPD structure, PEG is conjugated with a lipid anchor via a peptide targeted by matrix metalloproteinases, which are highly expressed in a broad range of cancers. The PEG chain is removed in tumor tissue in response to matrix metalloproteinases whereas PPD behaves like normal PEG in the blood. Conversely, shGALA is a pH-sensitive fusogenic peptide, whose sequence is optimized for *in vivo* tumor targeting. As shGALA has a characteristic repeat sequence, including a protonable glutamic acid, the structure of shGALA changes from a random coil to an α-helix in an acidic compartment of a cell, such as endosomes and lysosomes. Therefore, the fusogenic ability of shGALA caused by the hydrophobicity conferred by the α-helix form is able to overcome the inhibitory effect of PEG on endosomal escape. As these systems contained DOTAP that is a popular cationic lipid used for *in vitro* transfections,[20] a large degree of PEG modification was necessary for targeting a tumor via the EPR effect. In fact, these devices improve the endosomal escape ability of a PEG-modified MEND. To propose an alternate approach for overcoming the issue caused by PEGylation instead of a peptide-based solution, we reported on the possibility of using a newly designed cationic lipid, YSK05. The effect of PEGylation on liposomes composed of the conventional lipid, DOTAP, or YSK05 on fusion activity was evaluated to verify that YSK05 had suitable properties for tumor targeting, when intravenously injected. When liposomes were modified with a sufficient level of PEG to stably circulate in the blood stream, a 5% PEG-modified YSK05 liposome had a higher membrane fusion ability than a 15% PEG-modified DOTAP liposome (**Supplementary Figure S4**).

Despite the high transfection ability of the previously optimized YSK05-MEND for intratumoral injection, no silencing activity was observed in the liver after systemic injection (**Supplementary Figure S2a**). The injection of liposomes containing phosphoethanolamine can activate a complement cascade via alternative pathways, and consequently the binding of complement protein to the surface of liposomes should enhance their incorporation into macrophages.[16,21] These reports suggest that an optimized POPE-based MEND would be taken up by liver macrophages, kupffer cells, and hence, would not be able to deliver siRNA to hepatocytes. Similarly, tumor tissue contains high levels of tumor-associated macrophages.[22] The POPE-based MEND failed to decrease the target gene expression in tumor tissue, possibly due to the fact that large amounts were incorporated into these macrophages.

We previously reported that when tumor-bearing mice were injected with 4 mg/kg of shGALA-modified, DOTAP-based

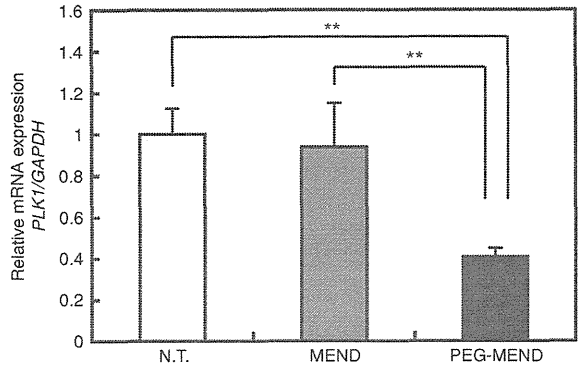

Figure 4 Comparison between the MEND and PEG-MEND on gene-silencing activity. *PLK1* mRNA expression was quantified 24 hours after the systemic injection of the MENDs into the tumor-bearing mice at a dose of 4 mg siRNA/kg bodyweight. The data are represented as the mean ± SD ($n = 3$). $^{**}P < 0.01$ (by one-way nrANOVA, followed by Student Newman-Keuls correction). ANOVA, analysis of variance; MEND, multifunctional envelope-type nanodevice; N.T., nontreatment; PEG, polyethylene glycol.

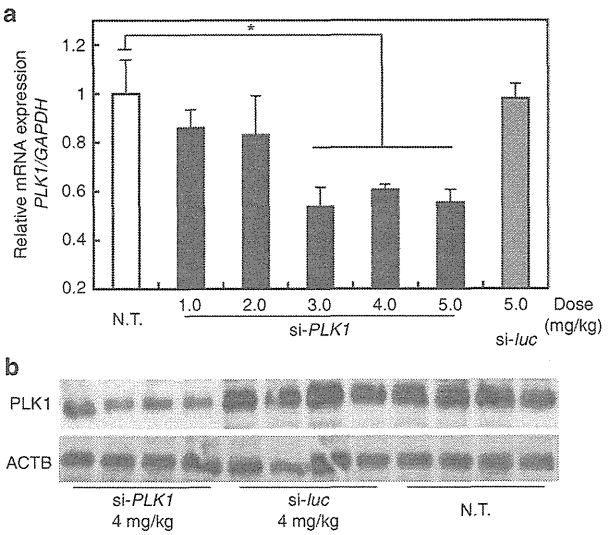

Figure 5 Gene-silencing effect of PEG-MEND. (**a**) mRNA level were measured with qRT-PCR and (**b**) PLK1 protein expression was determined by western blotting. PEG-MEND was injected into the tumor-bearing mice at various dosages. $^{*}P < 0.05$ (by one-way nrANOVA, followed by Bonferroni correction, versus N.T.). ANOVA, analysis of variance; MEND, multifunctional envelope-type nanodevice; N.T., nontreatment; PEG, polyethylene glycol; qRT-PCR, quantitative reverse transcriptase PCR.

MEND four times via the tail vein, a significant silencing of the target gene in tumor tissue somehow occurred. Conversely, just once injection of the YSK05-based MEND at 4 mg/kg demonstrated a significant target gene reduction. Taken together, these findings suggest that the DSPC-based YSK05-MEND has more appropriate properties for targeting tumors after systemic injection through the EPR effect than the DOTAP-based MEND.

First, the *in vitro* and *in vivo* properties of the MEND and PEG-MEND were evaluated. The siRNA formulated in MENDs was stable in fresh mouse serum for a period of up to 48 hours, but not in the presence of Triton X-100. The siRNA and lipid envelope formulated in the PEG-MEND circulated in the blood stream even 24 hours after the administration in RI experiments, whereas those formulated in the MEND did not, despite the stability of siRNA formulated in MEND against mice serum. These results show that only the PEG-MEND was able to exploit the EPR effect for the delivery of siRNA to tumor tissue. When a similar RI experiment was performed to measure the amounts of siRNA that accumulated in tumor tissue, unexpectedly high amounts of siRNA were detected in spite of the low lipid content of the MEND (**Figure 3a** and **Supplementary Figure S4**). As it has been previously reported that naked siRNA was unstable in blood,[23] and consequently, should not be delivered to tumor tissue, this result with RIs is likely to be artificial. Thus, to clarify the cause of the discrepancy in lipid and siRNA accumulation, we investigated the biodistribution of [^{32}P]-labeled naked siRNA after systemic administration (**Supplementary Figure S5**). A high [^{32}P] count was detected in liver, lungs, and tumor, unlike a previous report (**Supplementary Figure S6**).[23] In this latter report, in contrast to our results, the authors reported that siRNA did not accumulate in those organs in a full length, as evidenced by a northern blotting analysis. Therefore, there is a strong possibility that a catabolite of the labeled siRNA was detected in our RI experiment on siRNA biodistribution study.

Then, to precisely determine the amount of siRNA that accumulated in tumors, we performed stem-loop primer-mediated qRT-PCR, because this method selectively detects full-length siRNA.[12] The results show that the PEG-MEND delivered 240-fold more siRNA than the MEND (**Figure 3b**). Furthermore, in the confocal laser scanning microscopy data, a high degree of fluorescent signal of siRNA was detected in the tumor tissue treated with the PEG-MEND, but not in the mice treated with the MEND (**Figure 3c–e**). In the case of normal organs, the use of stem-loop primer qRT-PCR showed that free siRNA did not accumulate in the liver, spleen, kidney, and lung at all, which is consistent with a previous report (**Supplementary Figure S7**). In addition, the siRNA distribution with stem-loop primer data was more similar to the biodistribution of the lipid envelop distribution than that with the radio activity. These results suggest that experiments on organ distribution of siRNA with RIs include artifacts, and therefore, the stem-loop qRT-PCR is a more valid procedure for the quantitative evaluation of siRNA accumulation not only in liver but also in tumors and other organs.

In terms of mRNA knockdown, the PEG-MEND resulted in about a 60% reduction in the target gene mRNA expression, whereas MEND failed to show any gene-knockdown effect. This result indicates that the improvement of siRNA accumulation in tumor tissue was directly involved with the gene-silencing activity in tumors. Then, we quantitatively analyzed the efficiency of siRNA knockdown in tumor tissue. As 1 g of tumor tissue was estimated to contain $1.0 \times 10^8 - 10^9$ cells,[24] the number of siRNA molecules in a single cancer cell is calculated to be $7.0 \times 10^4 - 10^5$ molecule/cell. This estimated value was far higher than the value reported by Landesman *et al.* to achieve a 50% knockdown of the target mRNA in rat liver (~500 molecules/cell). The difference in knockdown efficacy must be the result of the efficiency of the siRNA, the type of target gene, lipid composition, and related factors. One of the

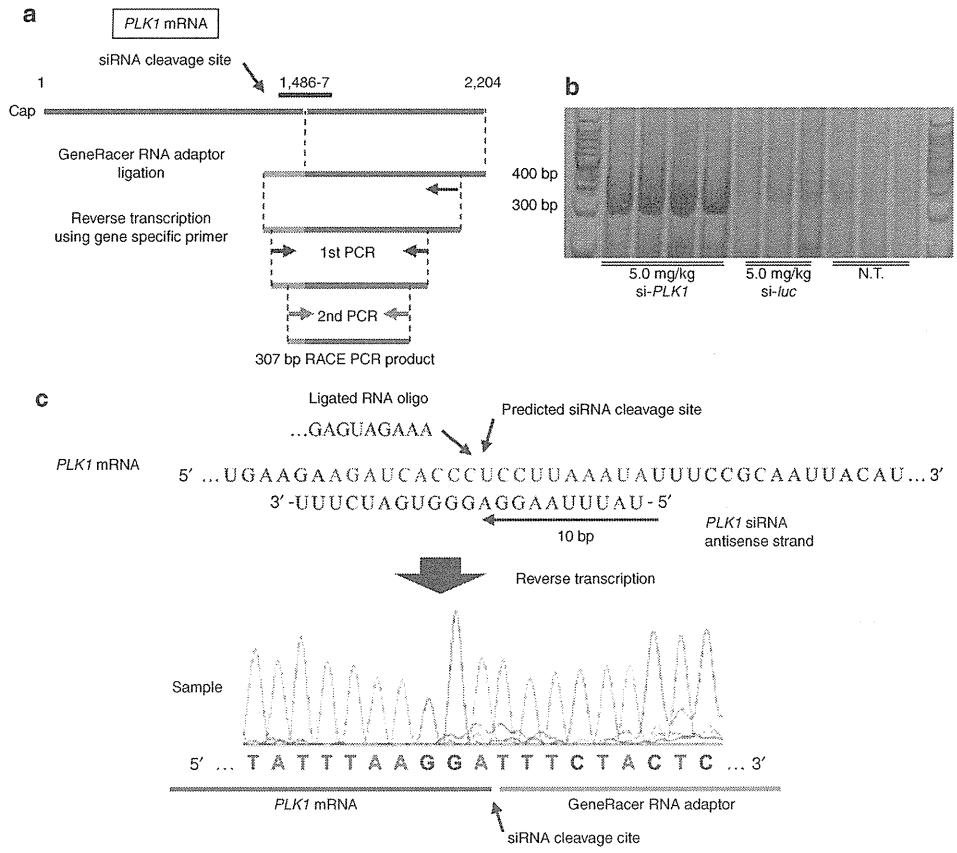

Figure 6 Confirming RNA interference. (**a**) The outline of 5′ RACE-PCR method for *PLK1* mRNA cleavage. Cleaved *PLK1* mRNA resulted in the 307 bp nested PCR products. (**b**) An actual result of electrophoresis of nested PCR products. (**c**) Predicted sequence of nested PCR product around siRNA cleavage site and the actual result of sequencing the PCR fragment. N.T., nontreatment.

major factors contributing to this difference might be the acyl chain moiety of the PEG-lipid. It was reported that the fusion ability of PEGylated liposomes decreased with the increasing length of the acyl chain moiety, because the higher was the rate of elimination out of the liposome membrane, the shorter was the acyl chain.[25,26] In the delivery of nucleic acids, the length of the acyl chain is also important. For example, Mok *et al.* reported 30-fold higher transfection levels when a plasmid DNA encapsulated cationic liposome with a C_8 PEG-lipid was achieved, compared with that with C_{14} PEG-lipid.[27] The endosome escape ability of the PEG-MEND should be relatively low, because the C_{18} PEG-lipid was used in our study. In contrast, the C_{14} PEG-lipid was used in Landesman's study. This issue is specific to passive tumor targeting system via EPR effect requiring a prolonged circulation of the carrier, and consequently, must make siRNA delivery more difficult than liver.

Concerning the dose dependency, the gene-knockdown efficacy reached a plateau at 3 mg/kg. This saturation might be caused by a restricted distribution of siRNA in tumor tissue. Actually, the tumor distribution of the siRNA formulated in the PEG-MEND appeared to be limited from the point of view of the confocal laser scanning microscopy results (**Figure 3e**). The diffusion of anticancer medicine in tumor tissue is more difficult than that for a normal organ because of the abundant extracellular matrix, a long distance from vessels and cancer cells, and a high interstitial fluid pressure.[28] The limitation in the tumor distribution is also applicable to nano-sized carriers. Cabral *et al.* reported that small micelles (30 nm in diameter) containing (1,2-diaminocyclo hexane)platinum(II) are spread over the entire tumor tissue, whereas large micelles (100 nm in diameter) remained near the tumor vessels.[29] Therefore, the size of the PEG-MEND would be a rate-determining step in gene reduction by siRNA in tumor tissue, and consequently, a decrease in PEG-MEND diameter can overcome the saturation in the RNAi effect.

Inhibition of the *PLK1* gene is known to have the potential to suppress the growth of cells in a wide range of cancers.[15] In renal cell carcinomas, a low-molecule weight inhibitor of PLK1 likewise also delayed the growth, both *in vitro* and *in vivo*,[30] and hence, it is logical to regard si-*PLK1* as a therapeutic gene against one of renal cell carcinoma cell lines, namely, OS-RC-2 cells. Unexpectedly, the continuous inhibition of *PLK1* for a 2-week period failed to inhibit OS-RC 2 tumor growth (data not shown). It is true that *PLK1* is a well-known representative anticancer gene, but *PLK1* knockdown by Lipofectamine 2000 showed a weaker effect on cell viability in OS-RC-2 cells (IC_{50} of viability; 100 nmol/l, IC_{50} of *PLK1* mRNA; 0.1 nmol/l) than in another cell line (IC_{50} of viability; 10 nmol/l, IC_{50} of *PLK1* mRNA; 2 nmol/l in HeLa cell). Further studies directed toward the elucidation of an appropriate gene for killing renal cell carcinomas will be required for renal

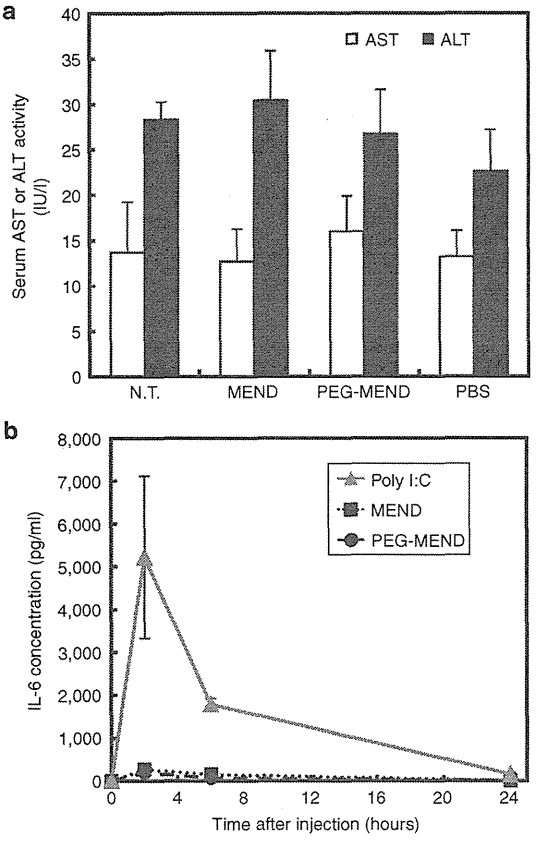

Figure 7 Toxicological analyses of injected MENDs. (**a**) Liver toxicity was evaluated by measuring AST and ALT activities in serum 6 hours after injection of each sample. (**b**) Immunostimulatory effect of injected MEND was evaluated by measuring IL-6 in serum. Poly I:C of 4 mg/kg of was used as an immunostimulatory oligonucleotide. IL-6 concentration was determined by ELISA at each time point. ALT, alanine aminotransferase; AST, asparate aminotransferase; MEND, multifunctional envelope-type nanodevice; N.T., nontreatment; PEG, polyethylene glycol.

cell cancer treatment. In terms of the toxicity of MENDs, in both groups treated with MENDs, a much lower amount of IL-6 was detected than in the poly I:C group (**Figure 7b**) though inflammatory cytokine production was investigated because it has been reported that siRNA has an immunostimulatory effect, as it is recognized by the TLRs 3, 7, and 8 or RIG-I.[31] The weak effect on an innate immune system might be attributed to the low accumulation in spleen and the high fusion ability of YSK05. Both MENDs were mostly distributed in liver, little in spleen (**Supplementary Figure S8**). Splenocyte captures liposome and removes it from blood stream, and consequently produces inflammatory cytokines by recognizing extrinsic substances, such as nucleic acids.[32] Followed by accumulation in immune cell, endosomal acidification and maturation are required for TLR expression. In fact, chroloquin treatment that caused a destruction of endosomes could decrease cytokine production in murine dendric cells.[33] Therefore, YSK05 might enable siRNA to escape before TLR maturation from endosomes and avoid being recognized by TLR, and consequently, could result in a low reduction of IL-6. This result suggests that both MENDs are likely to be safe siRNA carriers in terms of the absence of liver toxicity but also immune stimulation.

In conclusion, a MEND composed of YSK05 was used to deliver siRNA to tumor tissue by intravenous injection and to inhibit mRNA and protein expression of the target gene at a sufficient dose to permit its experimental use. Moreover, no adverse effects, such as liver toxicity and immunostimulation, were observed for the PEG-MEND. Collectively, an appropriately prepared MEND can be a novel tool for the investigations of the *in vivo* molecular biology of cancer and remains a viable basic technology for serving as an siRNA medicine in the future.

MATERIALS AND METHODS

Materials. DSPC; 1,2-dimyristoyl-sn-glycerol, methoxypolyethylene glycol (PEG_{2000}-DMG); and 1,2-Distearoyl-sn-glycerol, methoxypolyethylene glycol (PEG_{2000}-DSG) were purchased from NOF corporation (Tokyo, Japan). Cholesterol was obtained by SIGMA (St Louis, MO). [^{3}H]-cholesteryl-hexadecyl ether was purchased from PerkinElmer Life Sciences (Tokyo, Japan). YSK05 was synthesized and purified as previously reported.[11] siRNAs were purchased from Hokkaido System Science (Sapporo, Japan), and the sequences of siRNAs in the reports were shown in **Supplementary Table S1**. OS-RC-2 human renal cell carcinoma cells were kindly provided by K Hida (Hokkaido University, Sapporo, Hokkaido, Japan).

MEND preparation and characterization. The MEND was prepared as previously reported.[11] Briefly, an siRNA solution was added to an alcohol solution, in which YSK05, cholesterol, DSPC, and PEG_{2000}-DMG (50/40/10/0.03; mol% of total lipid) were dissolved. The alcohol was then removed by ultrafiltration through an Amicon system (MWCO 50,000; Millipore, Billerica, MA). The MEND was next incubated with 5 mol% of PEG_{2000}-DSG in a 10% ethanol solution for PEGylation. Ethanol was again removed using the Amicon system (Millipore). The z-average and the ζ-potential were determined using a Zetasizer Nano ZA ZEN3600 (MALVERN Instrument, Worchestershire, UK).

Serum resistance assay. Free or lipid-formulated siRNA (0.2 mg/ml) were incubated in 90% (v/v) mouse serum volume at 37 °C up to 48 hours in the presence or the absence of 0.1% Triton X-100. siRNA was extracted from serum using acid phenol/chloroform method. Aliquots containing 22 ng siRNA of each sample were loaded onto a 20% polyacrylamide gel, and electrophoresis was performed to visualize the intact siRNA. Mouse serum obtained within 6 hours was used for this assay.

Animal study and preparing tumor-bearing mice. Male ICR mice (4 weeks old) were obtained from Japan SLC (Shizuoka, Japan). For preparing tumor-bearing mice, OS-RC-2 cells (Riken Cell Bank, Tsukuba, Japan) were cultured in RPMI-1640 supplemented with 10% fetal bovine serum, penicillin (100 U/ml), and streptomycin (100 μg/ml) at 37 °C in a 5% CO_2 atmosphere. OS-RC-2 cells (1×10^6 cells) in 70 μl phosphate-buffered saline were subcutaneously injected into male BALB/cAJcl-*nu*/*nu* mice (CLEA Japan, Tokyo, Japan) on the right flank, and then grown until the tumor volume was 80–150 mm^3. The experimental protocols were reviewed and approved by the Hokkaido University Animal Care Committee in accordance with the guidelines for the care and use of laboratory animals.

Analysis of plasma concentration profiles and biodistribution of siRNA and the lipid envelope. The biodistribution of lipid and siRNA were measured with RIs, [^{3}H] and [^{32}P], respectively. The lipid envelope was labeled with [^{3}H]-cholesteryl-hexadecyl ether and [^{32}P]-phosphorylated siRNA was prepared, as previously reported.[10] RI-labeled MENDs were formulated by partially replacing components with RI-labeled ones in the preparation. The RI-labeled MEND was injected into ICR mice intravenously, and blood, liver, spleen, kidney, lung, and tumor were then collected. Serum was obtained by centrifugation. Approximately 0.1 g of each organ

was lysed in Soluene-350 (PerkinElmer) at 50 °C over night, and 10 ml of Hionic Fluor (PerkinElmer) was added to lysate. RI counts of these samples were measured using an LSC-6100 (ALOKA, Tokyo, Japan).

siRNA quantification with stem-loop PCR. siRNA quantification using a previously reported method.[12,34] Frozen tumor tissue that was weighed in advance was directly added into 500 µl of 0.25% Triton X-100 at 95 °C. The tumor tissue was then homogenized with PreCellys (Bertin Technologies, Montigny-le-Bretonneux, France). For preparing standard curves, known amounts of serially diluted siRNA were added to the tissue homogeneate from the non-treatment group.

Reverse transcription reactions were performed with TaqMan MicroRNA Reverse Transcription kit (Applied Biosystems, Carlsbad, CA). Tumor tissue homogeneates were heated at 95 °C for 10 minutes. Then, 5 µl of each sample was directly added into 10 µl of the reverse transcription mixture which was placed at 4 °C beforehand, and the reverse transcription program was started (16 °C × 30 minutes, 42 °C × 30 minutes, and 85 °C × 30 minutes). cDNA of 2 µl of was mixed with 7 µl of deionized distilled water, 1 µl of 20× Probe and Primer set, and 10 µl of 2× TaqMan PCR Master Mix, No AmpErase UNG (Applied Biosystems). The PCR parameters consisted of a primary denaturing at 95 °C × 10 minutes, followed by 40 cycles of PCR at 95 °C × 15 seconds, 60 °C × 1 minutes with LightCycler 480 II System (Roche Diagnostics GmbH, Germany).

Confocal laser scanning microscopy study. MENDs encapsulating Cy5-labeled siRNA were injected into tumor-bearing mice. Isolectin B4 of 50 µg of was intravenously injected into the tumor-bearing mice to visualize endothelial cells 10 minutes before collection, and then tumor tissue was excised. Thick tumor sections of 16 µm were prepared using a cryostat (CM3000; Leica, Tubingen, Germany), and then tissue images were obtained by FV10i (Olympus, Tokyo, Japan).

Gene expression analysis in tumor tissue. Tumor tissue was broken with Precellys and total RNA was purified with TRIzol (Ambion, Austin, TX) according to the manufacturer's protocol. A total RNA of 1 µg was reverse-transcribed with a RNA-to-cDNA Reverse Transcription Kit (Applied Biosystems) and 5 µl of 50 times diluted cDNA was then subjected to PCR amplification with 2× Fast SYBR Green Master Mix (Applied Biosystems) and 500 nmol/l of forward and reverse primer sets, whose sequences were shown in **Supplementary Table S2.** Relative *PLK1* mRNA amount was calculated with ddCt method and normalized to *GAPDH* mRNA amount.

Western blot analysis for protein expression in tumor tissue. Tumor tissue was lysed in RIPA buffer with Halt Protease Inhibitor Single-Use Cocktail (Thermo Fisher Scientific, Waltham, MA) on ice. The protein concentration in the tumor lysate was measured with BCA Protein Assay Reagent (Thermo Fisher Scientific), and then 2 µg aliquots of protein were subjected to SDS-PAGE. Mouse monoclonal anti-PLK1 antibody (WH0005347M1-100UG; SIGMA Aldrich) and anti-ACTB antibody (sc-130301; Santa Cruz Biotechnology, Santa Cruz, CA) were used as the first antibody, and ECL Antimouse IgG, Horseradish peroxidase-linked species-specific $F(ab')_2$ fragment was used as the second antibody.

RNAi confirmation with 5′ RLM RACE-PCR method. Rapid amplification of cDNA 5′ ends (5′ RACE)-PCR was performed referring to Gene Racer protocol and previous reports.[17,35] First, GeneRacer Adaptor, in which the 5′ ends were aminated to avoid self-ligation, was ligated into all RNA species in total RNA solution extracted from tumor homogenate with T4 RNA ligase (Ambion). Then *PLK1* mRNA was subjected to reverse transcribing using *PLK1* specific reverse transcription primer. PCR primer sets were designed against the ligated RNA oligo and the mRNA sequence lower than the expected siRNA cleavage site (Ad5 outer primer and *PLK1* outer primer). To obtain the PCR amplicon derived from cleaved target mRNA specifically, a second PCR was performed with primer sets against the inner site rather than the first PCR (nested PCR; Ad5 inner primer and *PLK1* inner primer). Nested PCR products were subjected to 10% TBE-polyacrylamide gel electrophoresis. The nested PCR amplicon band corresponding to mRNA cleavage was extracted from the polyacrylamide gel using QIAquick Gel Extraction Kit (QIAGEN, Hilden, Germany), and then sequenced with ABI 3130 system using the *PLK1* sequencing primer. The sequences of oligonucleotides used in this experiment were shown in **Supplementary Table S2.**

Toxicological test. Mice were intravenously injected with siRNA formulated in MENDs at a dose of 4 mg siRNA/kg body weight once. Blood samples were collected at various time points and allowed to stand at 4 °C for coagulation. Serum was obtained by centrifuging the coagulated blood at 3,000 rpm at 4 °C for 30 minutes. Cytokine levels were determined using an Enzyme linked Immunosorbent assay (ELISA) kit for IL-6 (R&D, Minneapolis, MN). Serum alanine transaminase and aspirate amino transferase activities were determined using a commercially available kit (Wako Chemicals, Osaka, Japan).

Statistical analysis. Comparisons between multiple treatments were made using one-way analysis of variance, followed by the Bonferroni test. Pairwise comparisons between treatments were made using the Student's *t*-test. A P value of <0.05 was considered to be significant.

SUPPLEMENTARY MATERIAL

Figure S1. Structural information for YSK05. Structural formula of the pH-sensitive cationic lipid, YSK05, whose IUPAC name is 1-methyl-4,4-bis[[9Z,12Z]-ocatadeca-9,12-dien-1-yloxy]piperidine.
Figure S2. Gene-silencing effect of MENDs in liver and tumor.
Figure S3. Comparison between YSK05 and conventional cationic lipid, DOTAP.
Figure S4. The fusogenic ability of YSK liposome and DOTAP liposome was determined by means of a hemolysis assay.
Figure S5. [^{32}P] accumulation in tumor tissue.
Figure S6. The biodistribution of systemically injected free [^{32}P]-siRNA.
Figure S7. Comparison of the methodology between radio isotope and stem-loop qRT-PCR methods.
Figure S8. The biodistribution of systemically injected [^{3}H]-cholesteryl-hexadecyl ether–labeled MEND and PEG-MEND.
Table S1. Pharamacokinetics parameters of siRNA encapsulated in MENDs.
Table S2. Sequences of oligonucleotides.

ACKNOWLEDGMENTS

This study was supported in part by a grant-in-aid for Young Scientists (B) from the Japan Society for the Promotion of Science (JSPS), the Special Education and Research Expenses of the Ministry of Education, Culture, Sports, Science, and Technology (MEXT) of Japan, a grant-in-aid for Scientific Research on Innovative Areas "Nanomedicine Molecular Science" (No. 2306) from MEXT of Japan, and by a grant for Industrial Technology Research from New Energy and Industrial Technology Development Organization (NEDO). The authors declare no conflict of interest.

REFERENCES

1. Burnett, JC and Rossi, JJ (2012). RNA-based therapeutics: current progress and future prospects. *Chem Biol* **19**: 60–71.
2. Castanotto, D and Rossi, JJ (2009). The promises and pitfalls of RNA-interference-based therapeutics. *Nature* **457**: 426–433.
3. Whitehead, KA, Langer, R and Anderson, DG (2009). Knocking down barriers: advances in siRNA delivery. *Nat Rev Drug Discov* **8**: 129–138.
4. Shim, MS and Kwon, YJ (2010). Efficient and targeted delivery of siRNA in vivo. *FEBS J* **277**: 4814–4827.
5. Kogure, K, Akita, H, Yamada, Y and Harashima, H (2008). Multifunctional envelope-type nano device (MEND) as a non-viral gene delivery system. *Adv Drug Deliv Rev* **60**: 559–571.
6. Maeda, H, Matsumura, Y and Kato, H (1988). Purification and identification of [hydroxyprolyl3]bradykinin in ascitic fluid from a patient with gastric cancer. *J Biol Chem* **263**: 16051–16054.

7. Ozpolat, B, Sood, AK and Lopez-Berestein, G (2010). Nanomedicine based approaches for the delivery of siRNA in cancer. *J Intern Med* **267**: 44–53.
8. Hatakeyama, H, Akita, H and Harashima, H (2011). A multifunctional envelope type nano device (MEND) for gene delivery to tumours based on the EPR effect: a strategy for overcoming the PEG dilemma. *Adv Drug Deliv Rev* **63**: 152–160.
9. Hatakeyama, H, Akita, H, Ito, E, Hayashi, Y, Oishi, M, Nagasaki, Y *et al.* (2011). Systemic delivery of siRNA to tumors using a lipid nanoparticle containing a tumor-specific cleavable PEG-lipid. *Biomaterials* **32**: 4306–4316.
10. Sakurai, Y, Hatakeyama, H, Sato, Y, Akita, H, Takayama, K, Kobayashi, S *et al.* (2011). Endosomal escape and the knockdown efficiency of liposomal-siRNA by the fusogenic peptide shGALA. *Biomaterials* **32**: 5733–5742.
11. Sato, Y, Hatakeyama, H, Sakurai, Y, Hyodo, M, Akita, H and Harashima, H (2012). A pH-sensitive cationic lipid facilitates the delivery of liposomal siRNA and gene silencing activity *in vitro* and in vivo. *J Control Release* **163**: 267–276.
12. Landesman, Y, Svrzikapa, N, Cognetta, A 3rd, Zhang, X, Bettencourt, BR, Kuchimanchi, S *et al.* (2010). *In vivo* quantification of formulated and chemically modified small interfering RNA by heating-in-Triton quantitative reverse transcription polymerase chain reaction (HIT qRT-PCR). *Silence* **1**: 16.
13. Jackson, AL and Linsley, PS (2010). Recognizing and avoiding siRNA off-target effects for target identification and therapeutic application. *Nat Rev Drug Discov* **9**: 57–67.
14. Kleinman, ME, Yamada, K, Takeda, A, Chandrasekaran, V, Nozaki, M, Baffi, JZ *et al.* (2008). Sequence- and target-independent angiogenesis suppression by siRNA via TLR3. *Nature* **452**: 591–597.
15. Lens, SM, Voest, EE and Medema, RH (2010). Shared and separate functions of polo-like kinases and aurora kinases in cancer. *Nat Rev Cancer* **10**: 825–841.
16. Patel, HM and Moghimi, SM (1998). Serum-mediated recognition of liposomes by phagocytic cells of the reticuloendothelial system - The concept of tissue specificity. *Adv Drug Deliv Rev* **32**: 45–60.
17. Judge, AD, Robbins, M, Tavakoli, I, Levi, J, Hu, L, Fronda, A *et al.* (2009). Confirming the RNAi-mediated mechanism of action of siRNA-based cancer therapeutics in mice. *J Clin Invest* **119**: 661–673.
18. Robbins, M, Judge, A, Ambegia, E, Choi, C, Yaworski, E, Palmer, L *et al.* (2008). Misinterpreting the therapeutic effects of small interfering RNA caused by immune stimulation. *Hum Gene Ther* **19**: 991–999.
19. Hatakeyama, H, Akita, H, Kogure, K, Oishi, M, Nagasaki, Y, Kihira, Y *et al.* (2007). Development of a novel systemic gene delivery system for cancer therapy with a tumor-specific cleavable PEG-lipid. *Gene Ther* **14**: 68–77.
20. Simberg, D, Weisman, S, Talmon, Y and Barenholz, Y (2004). DOTAP (and other cationic lipids): chemistry, biophysics, and transfection. *Crit Rev Ther Drug Carrier Syst* **21**: 257–317.
21. Moghimi, SM and Hunter, AC (2001). Recognition by macrophages and liver cells of opsonized phospholipid vesicles and phospholipid headgroups. *Pharm Res* **18**: 1–8.
22. Joyce, JA and Pollard, JW (2009). Microenvironmental regulation of metastasis. *Nat Rev Cancer* **9**: 239–252.
23. Gao, S, Dagnaes-Hansen, F, Nielsen, EJ, Wengel, J, Besenbacher, F, Howard, KA *et al.* (2009). The effect of chemical modification and nanoparticle formulation on stability and biodistribution of siRNA in mice. *Mol Ther* **17**: 1225–1233.
24. Del Monte, U (2009). Does the cell number 10(9) still really fit one gram of tumor tissue? *Cell Cycle* **8**: 505–506.
25. Holland, JW, Hui, C, Cullis, PR and Madden, TD (1996). Poly(ethylene glycol)-lipid conjugates regulate the calcium-induced fusion of liposomes composed of phosphatidylethanolamine and phosphatidylserine. *Biochemistry* **35**: 2618–2624.
26. Silvius, JR and Zuckermann, MJ (1993). Interbilayer transfer of phospholipid-anchored macromolecules via monomer diffusion. *Biochemistry* **32**: 3153–3161.
27. Mok, KW, Lam, AM and Cullis, PR (1999). Stabilized plasmid-lipid particles: factors influencing plasmid entrapment and transfection properties. *Biochim Biophys Acta* **1419**: 137–150.
28. Heldin, CH, Rubin, K, Pietras, K and Ostman, A (2004). High interstitial fluid pressure - an obstacle in cancer therapy. *Nat Rev Cancer* **4**: 806–813.
29. Cabral, H, Matsumoto, Y, Mizuno, K, Chen, Q, Murakami, M, Kimura, M *et al.* (2011). Accumulation of sub-100 nm polymeric micelles in poorly permeable tumours depends on size. *Nat Nanotechnol* **6**: 815–823.
30. Ding, Y, Huang, D, Zhang, Z, Smith, J, Petillo, D, Looyenga, BD *et al.* (2011). Combined gene expression profiling and RNAi screening in clear cell renal cell carcinoma identify PLK1 and other therapeutic kinase targets. *Cancer Res* **71**: 5225–5234.
31. Robbins, M, Judge, A and MacLachlan, I (2009). siRNA and innate immunity. *Oligonucleotides* **19**: 89–102.
32. Wilson, KD, de Jong, SD and Tam, YK (2009). Lipid-based delivery of CpG oligonucleotides enhances immunotherapeutic efficacy. *Adv Drug Deliv Rev* **61**: 233–242.
33. Diebold, SS, Kaisho, T, Hemmi, H, Akira, S and Reis e Sousa, C (2004). Innate antiviral responses by means of TLR7-mediated recognition of single-stranded RNA. *Science* **303**: 1529–1531.
34. Cheng, A, Li, M, Liang, Y, Wang, Y, Wong, L, Chen, C *et al.* (2009). Stem-loop RT-PCR quantification of siRNAs *in vitro* and in vivo. *Oligonucleotides* **19**: 203–208.
35. Davis, ME, Zuckerman, JE, Choi, CH, Seligson, D, Tolcher, A, Alabi, CA *et al.* (2010). Evidence of RNAi in humans from systemically administered siRNA via targeted nanoparticles. *Nature* **464**: 1067–1070.

Lipids (2012) 47:1053–1062
DOI 10.1007/s11745-012-3716-8

ORIGINAL ARTICLE

High Serum Palmitic Acid is Associated with Low Antiviral Effects of Interferon-Based Therapy for Hepatitis C Virus

Teruki Miyake · Yoichi Hiasa · Masashi Hirooka · Yoshio Tokumoto · Takao Watanabe · Shinya Furukawa · Teruhisa Ueda · Shin Yamamoto · Teru Kumagi · Hiroaki Miyaoka · Masanori Abe · Bunzo Matsuura · Morikazu Onji

Received: 15 April 2012 / Accepted: 27 August 2012 / Published online: 16 September 2012

Abstract Hepatitis C virus (HCV) infection alters fatty acid synthesis and metabolism in association with HCV replication. The present study examined the effect of serum fatty acid composition on interferon (IFN)-based therapy. Fifty-five patients with HCV were enrolled and received IFN-based therapy. Patient characteristics, laboratory data (including fatty acids), and viral factors that could be associated with the anti-HCV effects of IFN-based therapy were evaluated. The effects of individual fatty acids on viral replication and IFN-based therapy were also examined in an in-vitro system. Multivariate logistic regression analysis showed that the level of serum palmitic acid before treatment and HCV genotype were significant predictors for rapid virological response (RVR), early virological response (EVR), and sustained virological response (SVR). High levels of palmitic acid inhibited the anti-HCV effects of IFN-based therapy. HCV replication assays confirmed the inhibitory effects of palmitic acid on anti-HCV therapy. The concentration of serum palmitic acid is an independent predictive factor for RVR, EVR, and SVR in IFN-based antiviral therapy. These results suggest that the effect of IFN-based antiviral therapy in patients with HCV infection might be enhanced by treatment that modulates palmitic acid levels.

Keywords Fatty acid · Hepatitis C virus · Interferon · Palmitic acid · Virological response

Abbreviations

AUC	Area under curve
BMI	Body mass index
DMEM	Dulbecco's modified Eagle's medium
EVR	Early virological response
GAPDH	Glyceraldehyde-3-phosphate dehydrogenase
HCC	Hepatocellular carcinoma
HBc	Hepatitis B core
HBs-Ag	Hepatitis B surface antigen
HBV	Hepatitis B virus
HCV	Hepatitis C virus
IFN	Interferon
IL-28B	Interleukin-28B
ISDR	Interferon sensitivity-determining region
NPV	Negative predictive value
NS5	Nonstructural-5
PEG-IFN	Pegylated interferon
PPV	Positive predictive value
RBV	Ribavirin
ROC	Receiver operating characteristics
RVR	Rapid virological response
SVR	Sustained virological response
PCR	Polymerase chain reaction

Introduction

Hepatitis C virus (HCV) infection is common worldwide, and more than 80 % of patients develop chronic infection.

Electronic supplementary material The online version of this article (doi:10.1007/s11745-012-3716-8) contains supplementary material, which is available to authorized users.

T. Miyake · Y. Hiasa (✉) · M. Hirooka · Y. Tokumoto · T. Watanabe · S. Furukawa · T. Ueda · S. Yamamoto · T. Kumagi · M. Abe · B. Matsuura · M. Onji
Department of Gastroenterology and Metabology, Ehime University Graduate School of Medicine, Toon, Ehime 791-0295, Japan
e-mail: hiasa@m.ehime-u.ac.jp

H. Miyaoka
Internal Medicine, Saiseikai Matsuyama Hospital, Matsuyama, Ehime 791-8026, Japan

Of those with chronic infection, 20–30 % develop cirrhosis and hepatocellular carcinoma (HCC) [1]. Interferon (IFN)-based treatment regimens have been widely used, but these treatment regimens have side effects, require long-term therapy, and are expensive. Estimation of the effectiveness of IFN-based therapy prior to treatment would be beneficial.

The velocity of decrease in viral load during IFN-based therapy is a good indicator for the prediction of sustained virological response (SVR). High SVR rates are predicted by rapid virological response (RVR) and early virological response (EVR) [2, 3]. Although mechanisms of treatment failure are poorly understood, previous reports have proposed IFN-stimulated genes and the inability to develop effective anti-HCV immunity as possible explanations [4].

Recently, fatty acids have been implicated in the pathogenesis of several diseases associated with metabolic disorders (such as obesity, diabetes and cardiovascular disease) [5, 6] and in immunological response [7]. In liver diseases, especially in non-alcoholic steatohepatitis, the effect of impaired peroxisomal polyunsaturated fatty acid metabolism and nonenzymatic oxidation on fatty acid constitution is associated with disease progression [8]. It has been reported that HCV core protein has effects on fatty acid synthesis, and that fatty droplets in the liver are related to development of disease [9, 10]. Although there have been reports about the role of fatty acids in liver in patients with HCV [9, 10], the relationship between serum fatty acids and efficacy of IFN-based antiviral therapy against HCV remains controversial.

The aims of the present study were to evaluate whether the composition of serum fatty acids could predict RVR, EVR, or SVR from IFN-based therapy in patients with HCV. Data from HCV patients were collected and in-vitro assays were performed using HCV-replication cell culture systems.

Patients and Methods

Patients

Consecutive patients with HCV treated with IFN-based therapy at Ehime University Hospital were enrolled prospectively from December 2008 to December 2010. Moreover, 10 healthy volunteers (age range 26–70 years) were enrolled in this study as healthy subjects. This study was carried out in accordance with the Declaration of Helsinki, and the institutional review board of Ehime University Hospital approved this study (Approval # 0710004). Written informed consent was provided by study participants.

Patients with chronic HCV infection, with creatinine clearance >50 mL/min, and who had not been previously treated with antiviral or immunosuppressive agents within the 3 months preceding enrollment were included. Patients with other liver disease such as autoimmune hepatitis, primary biliary cirrhosis, hepatitis B virus (HBV) infection, or HCC; co-infection with human immunodeficiency virus; poorly controlled cardiovascular, hematologic or pulmonary disease; pregnancy; autoimmune disease; severe depression or other psychiatric disorders; and/or active substance abuse were excluded. To exclude HBV infection, hepatitis B surface antigen (HBs-Ag) and anti-hepatitis B core (HBc) antibody were checked. Patients with positive HBs-Ag or a high titer of anti-HBc antibody were excluded.

Interferon and Ribavirin Combination Therapy

Patients received one of four treatment regimens: [1] pegylated interferon (PEG-IFN) α-2b 1.0 μg/kg/week or 1.5 μg/kg/week subcutaneously in combination with oral ribavirin (RBV) dosed by body weight (40–65 kg, 800 mg/day; >65–85 kg, 1,000 mg/day; >85–105 kg, 1,200 mg/day; >105–125 kg, 1,400 mg/day), [2] PEG-IFN α-2a 180 μg/week subcutaneously plus oral RBV dosed as above, [3] PEG-IFN α-2a 180 μg/week subcutaneously, or [4] IFN-β 600 million IU/day intravenously plus oral RBV dosed as above. In order to identify the levels of fatty acids that could have an important role in the response to treatment with IFN, all patients who had been treated with IFN were enrolled. After informing potential subjects about the costs, estimated adverse events, and effects of each treatment protocol according the Japanese guidelines for anti-HCV treatment [11], the required treatment regimen was chosen and treatment was started.

Laboratory Assessment

Patients' serum samples were collected around 6 a.m. after fasting on day 2 of the study before IFN-based treatment. Additionally, fasting serum was collected at the end of IFN-based treatment. Serum samples were frozen and stored at −80 °C within 4 h of collection and then thawed at the time of measurement. Fatty acid concentrations in total serum lipids was measured with liquid chromatography (SRL Co. Ltd., Tokyo, Japan). Subjects were diagnosed as having dyslipidemia if they had TC ≥220 mg/dL, and/or HDL-c ≤40 mg/dL, and/or TG ≥150 mg/dL [12], and/or taking lipid-lowering agents.

The HCV genotype was determined by the polymerase chain reaction (PCR) using a mixed primer set derived from nucleotide sequences from the nonstructural-5 (NS5) region (SRL Co. Ltd.) [13]. HCV RNA was measured quantitatively before and during therapy using PCR (Cobas Amplicor HCV monitor v 2.0 using the tenfold dilution method, Roche Diagnostics, Mannheim, Germany). The

lower level of detection for this assay was less than 1.2 $\log_{10}$ IU/mL. Undetectable serum HCV RNA on testing was considered a negative test. RVR was defined as undetectable serum HCV RNA within 4 weeks from the start of the treatment. EVR was defined as undetectable serum HCV RNA within 12 weeks from the start of the treatment. SVR was defined as undetectable serum HCV RNA within 24 weeks after the end of treatment.

The HCV genotype recovered from patients was determined using the Illumina Human610-quad BeadChip (Illumina, San Diego, CA, USA) as previously described [14, 15]. Amino acid substitutions of aa70 or aa91 in the core region of HCV genotype 1b were evaluated by agarose gel electrophoresis using mutation-specific primers for wild-type (aa70: arginine, aa91: leucine) and mutant (aa70: glutamine/histidine, aa91: methionine) viruses (SRL Co. Ltd.) [16]. In this study, the pattern of arginine (wild-type) at aa70 and leucine (wild-type) at aa91 was evaluated as double wild-type, while the other patterns were non-double wild-type. The nucleotide sequence of the interferon sensitivity-determining region (ISDR) in the HCV NS5A region was determined by direct sequencing through PCR-amplified materials [17]. Wild-type ISDR was defined as having no amino acid substitutions based on the HCV-J strain of genotype 1b.

Assay for Detecting Single Nucleotide Polymorphisms of Interleukin-28B (IL-28B)

Two single nucleotide polymorphisms of interleukin-28B (rs8099917 [14] and rs12979860 [15]) were examined using the TaqMan assay. The sequence of the probe and primers for the TaqMan assay for detecting rs8099917 was provided by Dr. Yasuhito Tanaka (Department of Virology and Liver Unit, Nagoya City University Graduate School of Medical Sciences, Nagoya, Japan), and rs12979860 was provided by Dr. David B. Goldstein (Center for Human Genome Variation, Duke University, Durham, NC, USA). Patient DNA was isolated from blood samples. For rs8099917 [14], homozygotes (T/T) were defined as having the IL-28B major allele, and heterozygotes (T/G) or homozygotes (G/G) were defined as having the minor allele. For rs12979860 [25], homozygotes (C/C) were defined as having the major allele, and heterozygotes (T/C) or homozygotes (T/T) were defined as having the minor allele.

Preparation of the In-Vitro Replication System

The human hepatoma cell lines Huh7 (Japanese Collection of Research Bioresources, Osaka, Japan) and Huh7.5.1 (provided by Dr. Francis V. Chisari; Department of Immunology and Microbial Science, The Scripps Research Institute, La Jolla, CA, USA) were cultured with Dulbecco's modified Eagle's medium (DMEM) (Sigma Chemical, St. Louis, MO, USA) containing 10 % fetal bovine serum (Filtron PTY LTD, Brooklyn, Australia).

For the in-vitro assay of HCV genotype 1, the plasmid-based binary HCV replication system was used [18, 19], in which the plasmid contained the infectious full-length genotype 1a cDNA sequence corresponding to the H77 prototype strain with the T7 promoter sequence (pT7-flHCV-Rz, provided by Dr. Raymond T. Chung (Gastrointestinal Unit, Massachusetts General Hospital, Boston, MA, USA). pT7-flHCV-Rz cells were transfected to Huh7 cells by using Lipofectamine (Invitrogen, Carlsbad, CA, USA). Subsequently, the T7 polymerase was delivered by using a replication-defective adenovirus vector (Ad-T7pol) at a multiplicity of infection of 10.

For the in-vitro assay of HCV genotype 2, the HCV replication system pJFH1-full that encodes HCV genotype 2a JFH1 sequence was used, which was provided by Dr. Takaji Wakita (Department of Virology II, National Institute of Infectious Diseases, Tokyo, Japan) [20]. HCV RNA was synthesized using the Megascript T7 kit (Ambion, Austin, TX, USA), with the linearized pJFH1-full as template. After DNase I (Ambion) treatment, the transcribed HCV RNA was purified using ISOGEN-LS (Nippon Gene, Tokyo, Japan). For RNA transfection, Huh 7.5.1 cells were resuspended in Opti-MEM I (Invitrogen) containing 10 μg of HCV RNA and subjected to an electric pulse (960 μF and 260 V) using the Gene Pulser II apparatus (Bio-Rad, Richmond, CA, USA). After electroporation, the cell suspension was cultured under normal conditions with DMEM.

Evaluation of Effect of Palmitic Acid In Vitro

For the in-vitro assay, palmitic acid (Sigma Chemical), myristic acid (Sigma Chemical), stearic acid (Sigma Chemical), and oleic acid (Sigma Chemical), were solubilized in ethanol with albumin as a stock solution of 20 mM and stored at −20 °C, as described previously [21, 22]. These fatty acid-albumin complex solutions were freshly prepared before each experiment. Subsequently, preliminary experiments were performed using 10–500 μM solutions of fatty acids in order to assess the concentrations of fatty acids that would not compromise cell viability. Cell viability was not compromised when 10–100 μM fatty acids were used in the MTS assay (cytotoxicity assay using 3-(4,5-dimethylthiazol-2-yl)-5-(3-carboxymethoxyphenyl)-2-(4-sulfophenyl)-2H-tetrazolium, CellTiter 96 Aqueous One Solution cell proliferation assay®, Promega, Madison, WI) [18]; thus, 100 μM fatty acids were used for culture experiments. Fatty acids were added after the preparation of H77 and JFH1 HCV replication cells, and then IFN-α2b

(100 IU/mL) and RBV (50 μM) were added to the culture medium of those cells. In the control samples, solubilized solutions were added without fatty acids.

Quantitative Real-Time Reverse-Transcription PCR

Cellular mRNA was extracted by TRIzol (Invitrogen), and levels of HCV replication were quantified by real-time reverse transcription-PCR with SYBR green I dye (Roche Diagnostics) and primers encoded for the 5′UTR of HCV using LightCycler technology (Roche Diagnostics) as described previously [18, 19]. Glyceraldehyde-3-phosphate dehydrogenase (GAPDH) (Roche Diagnostics) was detected using primer sets under the recommended conditions. Data are expressed as copy numbers of HCV RNA or cellular mRNA per molecule of GAPDH mRNA.

Statistical Analysis

Data are expressed as means ± standard deviations or as means ± standard errors of mean. The Wilcoxon test was used to analyze continuous variables. The Chi-square test was used for analysis of categorical data. Group comparisons involving more than two independent groups were performed using the Kruskal–Wallis test. Multivariate analysis was performed using a logistic regression model with stepwise method. The relationships between palmitic acid and the other parameters were analyzed with the Pearson product-moment correlation coefficient. Each cutoff point for continuous variables was decided by receiver operating characteristics (ROC) curve analysis. The RVR, EVR, and SVR rates of patients with low levels of palmitic acid were defined as positive predictive value (PPV) in the prediction of RVR, EVR, and SVR. Non-RVR, non-EVR, and non-SVR rates in patients with high levels of palmitic acid were defined as the negative predictive value (NPV) for prediction of non-RVR, non-EVR, and non-SVR. A P value of less than 0.05 was considered statistically significant. Statistical analyses were performed using JMP version 9 software (SAS Institute Japan, Tokyo, Japan).

Results

Patient Characteristics

A total of 55 patients with HCV were included. There were 27 men and 28 women. The mean age was 53.59 ± 11.15 years (range 22–69 years). The baseline characteristics of the study population are shown in Supplemental Table 1. Thirty-seven patients were infected with genotype 1 (all genotype 1b) and 18 patients with genotype 2 (14 with genotype 2a and four with genotype 2b). There was no significant difference between two groups in serum lipid composition (Table 1).

Response to Treatment

Among patients with genotype 1, 22 % (8/37) of patients received PEG-IFN α-2a plus RBV, 16 % (6/37) received PEG-IFN α-2a, 51 % (19/37) received PEG-IFN α-2b plus RBV, and 11 % (4/37) received IFN-β plus RBV. Among patients with genotype 2, 6 % (1/18) of patients received PEG-IFN α-2a plus RBV, 22 % (4/18) received PEG-IFN α-2a, 67 % (12/18) received PEG-IFN α-2b plus RBV, and 6 % (1/18) received IFN-β plus RBV.

RVR was achieved in 35 % (19/55) of patients overall. Twenty-seven percent (10/37) of patients with HCV genotype 1, and 50 % (9/18) with genotype 2 achieved RVR. EVR occurred in 64 % (35/55) of patients. EVR was achieved in 51 % (19/37) of patients with HCV genotype 1, and in 89 % (16/18) of patients with genotype 2.

For assessment of SVR, four patients dropped out of the treatment because of depression (2/4), general fatigue (3/4), and retinopathy (1/4). SVR was achieved in 69 % (35/51) of patients overall, in 56 % (19/34) of patients with HCV genotype 1, and in 94 % (16/17) of patients with genotype 2 evaluated by the above described protocol.

Predictors of Virological Response

Univariate analysis was performed for factors associated with RVR, EVR, and SVR (Supplemental Table 2). For RVR, a low serum triglyceride level was identified as a contributing factor. For EVR, low body mass index (BMI) and HCV genotype 2 were identified as contributing factors. For SVR, low BMI, total cholesterol, and HCV genotype 2 were identified as contributing factors. Further analysis was performed to examine the relationship of fatty acid levels to RVR, EVR, and SVR (Table 2). Table 2 shows the fatty acids significantly associated with virological response to IFN-based therapy by univariate analysis ($P < 0.05$). Other than the listed fatty acids, lauric acid, arachidic acid, behenic acid, lignoceric acid, myristoleic acid, eicosenoic acid, erucic acid, linoleic acid, γ-linolenic acid, arachidonic acid, and eicosapentaenoic acid were evaluated; however, those fatty acids were not significantly associated with any treatment response (RVR, EVR, or SVR). For RVR, low levels of myristic acid, palmitic acid, stearic acid, oleic acid, α-linolenic acid, eicosadienoic acid, adrenic acid, docosapentaenoic acid, and docosahexaenoic acid were identified as significant contributing factors. For EVR, palmitic acid and nervonic acid were identified as significant contributing factors. For SVR, myristic acid, palmitic acid, palmitoleic acid,